DESIGN AND OPTIMIZATION OF MICROSTSRIP PATCH ANTENNA USING DIFFERENTIAL EVOLUTION ALGORITHM FOR WIRELESS APPLICATIONS

A Dissertation Submitted in Partial Fulfillment of the Requirement for the Award of the Degree of

MASTER OF ENGINEERING

In

Electronics and Communication Engineering

Submitted By

NITIKA

Roll No. 801563018

Under Supervision of

Dr. Jaswinder Kaur

Assistant Professor, ECED

ELECTRONICS AND COMMUNICATION ENGINEERING DEPARTMENT

THAPAR UNIVERSITY, PATIALA, PUNJAB

JUNE, 2017

DECLARATION

I, Nitika hereby declare that the work presented in this thesis entitled "Design and Optimization of Microstrip Patch Antenna using Differential Evolution Algorithm for Wireless Applications" in partial fulfillment of the requirement for the award of degree of Master of Engineering submitted at Electronics and Communication Engineering Department, Thapar University, Patiala is an authentic record of work carried out under supervision of Dr. Jaswinder Kaur (Assistant Professor, ECED) from 2015 to 2017. The matter presented in this has not been submitted either in part or full to any other university or institute for the award of any other degree.

Date:...17/07/2017.....

(Nitika)
(801563018)

It is certified that the above statement made by the candidate is correct to the best of my knowledge and belief.

Date:...17/07/2017.....

Jaswinder Kaur 17/07/17

(Dr. Jaswinder Kaur)
(Assistant Professor, ECED)

ACKNOWLEDGEMENT

It is my proud privilege to acknowledge and extend my gratitude to several people who helped me directly or indirectly in completion of this report. I express my heart full indebtedness and owe a deep sense of gratitude to my teacher and my faculty guides **Dr. Jaswinder Kaur, Assistant Professor,** for their sincere guidance and support with encouragement to go ahead.

I am also thankful to **Dr. Alpana Agarwal**, Professor and Head, ECED, for providing us with the adequate infrastructure for carrying out the work. I am also thankful to **Dr. Hemdutt Joshi,** Associate Professor & P.G. Coordinator, ECED, for the motivation and inspiration and that triggered me for the work.

I would also like to thank my entire friends who have more or less contributed to the preparation of this report. Last but not the least, I would like to thank my parents for their years of unyielding love and encourage. They have always wanted the best for me and I admire their determination and sacrifice. The study has indeed helped me to explore knowledge and avenues related to my topic and I am sure it will help me in my future.

Nitika
(801563018)

ABSTRACT

Microstrip patch antennas have a lot of qualities like light weight, low profile, ease of fabrication and low production cost. These antennas have many applications such as spacecraft, high performance aircraft, missiles, and space satellites, where constraints are weight, size, performance, cost, aerodynamic profile, and ease of installation. There are many other applications like wireless communications and mobile radio which use microstrip antennas and hence, they play a very important role in this era of wireless communication systems. Antenna parameters need to be optimized for obtaining better results. Thus an algorithm technique is used for ease in computation complexity for optimizing different antenna parameters. Differential Evolution Algorithm is a strategy that optimizes a problem by utilizing iterative method to improve a candidate solution to a given measure of quality. This optimization technique improve the results by maintain a population of candidates solutions and developing new candidate solutions by combination of all presented ones according to its simple formulae and then considering the candidate solution with best score or fitness value. In this thesis work a hand-fan shaped, modified t-shape and dual-band rectangular MPAs are represented. A modified t-shape and dual-band rectangular MPAs were optimized using DE algorithm. The proposed antennas cover the frequency range of 2.34–2.68 GHz and 5.28–6.32 GHz with 340 MHz and 1040 MHz bandwidth respectively, 2.34–2.68 GHz and 5.28–6.32 GHz with their respective bandwidths of 690 MHz and 1120 MHz and 0.91 - 2.82 GHz with bandwidth of 1910 MHz.

TABLE OF CONTENTS

Sr. No	Name of the Chapters	Page No
	Declaration……..	*i*
	Acknowledgement……	*ii*
	Abstract…….	*iii*
	Table of Contents……	*iv*
	List of Tables……	*vii*
	List of Figures……..	*ix*
	List of Abbreviations……..	*x*
Chapter 1	Introduction……	*1-15*
1.1	Introduction…….	*1*
1.2	Microstrip Patch Antennas…….	*2-4*
1.2.1	Background……	*2*
1.2.2	Physical Configuration……	*2-4*
1.3	Antenna Properties……..	*4-5*
1.3.1	Gain…….	*4*
1.3.2	Voltage Standing Wave Ratio (VSWR)……..	*4-5*
1.3.3	Return Loss…….	*5*
1.4	Advantages and Disadvantages of Microstrip Patch Antenna…….	*5*
1.4.1	Advantages of MPAs……..	*5*
1.4.2	Disadvantages of MPAs……..	*5*
1.5	Microstrip patch antennas feed techniques……	*5-7*
1.5.1	Microstrip line feed technique……	*6*
1.5.2	Coaxial probe feed technique…….	*6*
1.5.3	Aperture coupled feed technique……...	*7*
1.5.4	Proximity coupled feed technique……..	*7*
1.6	Applications of Microstrip patch Antennas……	*8-9*

1.6.1	Mobile and Satellite communication applications…….	*8*
1.6.2	Global Positing System applications……...	*8*
1.6.3	Radio Frequency Identifier (RFID)…….	*8*
1.6.4	Worldwidea Inteoperability for microwave access (WiMAX)……	*9*
1.6.5	Radar applications……	*9*
1.7	Differential Evolution algorithm…….	*9-13*
1.7.1	History……	*9*
1.7.2	Overview……	*9*
1.7.3	Example of DE algorithm……..	*10-13*
1.8	Problem Statement…….	*13-14*
1.9	Research objectives and justification of study…….....	*14-15*
1.10	Organization of thesis……	*15*
Chapter 2	Literature Survey…….....	*16-19*
Chapter3	Design of Dual band MPA using DE for wireless applications…….....	*20-29*
3.1	Introduction……...	*20-21*
3.2	Antenna design and simulation with and without DE……..	*22-29*
3.2.1	Simulation results of S-parameters, VSWR and gain without DE……...	*23-25*
3.2.2	Simulation results of S-parameters, VSWR and gain with DE…….....	*25-27*
3.3.3	Current Distrubution of proposed antenna with DE……	*27-29*
Chapter 4	Design and optimization of modified t-shape MPA using DE for X and Ku applications	*30-36*
4.1	Introduction……	*30-31*
4.2	Antenna design and simulation with and without DE……..	*30-36*
4.2.1	Simulation results of S-parameters, VSWR and gain without DE……...	*32-33*
4.2.2	Simulation results of S-parameters, VSWR and gain with DE…….....	*33-34*
4.2.3	Current Distribution of proposed antenna with DE……	*35-36*
Chapter 5	Design of Hand-fan shaped MPA with U-slot DGS for L and S band applications...	*36-41*
5.1	Introduction……...	*37*
5.2	Antenna design and simulation…….	*37-41*
5.2.1	Simulation results of S-parameters, VSWR and gain…….……...	*38-40*
5.2.2	Current Distribution of proposed antenna……	*30-41*

Chapter 6 Fabrication and Testing of proposed antennas…… *42-49*

6.1 Fabrication procedure……... *42-43*

6.2 Testing of fabricated antennas……. *43*

6.3 Fabrication of Dual band MPA…… *43-45*

6.3.1 Comparison of simulated and measured results of proposed…… *44-45*

6.4 Fabrication of modified t-shape antenna…… *46-48*

6.4.1 Comparison of simulated and measured results of proposed…… *46-48*

6.5 Fabrication of hand-fan shaped antenna…… *48-49*

6.5.1 Comparison of simulated and measured results of proposed…… *49*

Chapter 5 Conclusion and Future scope……... *50-53*

References……... *54-56*

List of Publication…… *57*

LISTS OF TABLES

Sr. No	Table Details	Page No
Table 1.1	*Comparison of different Feed Techniques.....*	*8*
Table 1.2	*The intial population along with the objective function.....*	*11*
Table 1.3	*Calculation of Weighted Difference Vector.....*	*11*
Table 1.4	*Calculation of Noisy Random Vector.....*	*12*
Table 1.5	*Generation of the trial vector.....*	*12*
Table 1.6	*New population for next generation.....*	*13*
Table 3.1	*Specifications of proposed antenna.....*	*27*
Table 3.2	*Comparison of proposed antenna with and without optimization.....*	*27*
Table 4.1	*Comparison of proposed antenna with and without optimization.....*	*36*
Table 5.1	*Geometrical Configuration of proposed antenna.....*	*38*
Table 6.1	*Comparison of measured and simulated results of proposed antenna*	*48*

LISTS OF FIGURES

Sr. No	Figure Details	Page No
Figure 1.1	*Cross-Sectional View of a MPA*	*3*
Figure 1.2	*Representative Shapes of MPAs*	*3*
Figure 1.3	*Structure of Rectangular MPA*	*4*
Figure 1.4	*Microstrip Line Feed Technique*	*6*
Figure 1.5	*Coaxial Probe Feed Technique*	*6*
Figure 1.6	*Aperture-Coupled Feed Technique*	*7*
Figure 1.7	*Proximity-Coupled Feed Technique*	*7*
Figure 1.8	*Flowchart of DE Algorithm*	*9*
Figure 3.1	*Flowchart of DE Algorithm*	*21*
Figure 3.2	*Geometrical configuration of proposed antenna*	*22*
Figure 3.3	*Simulated reflection coefficient of proposed antenna*	*23*
Figure 3.4	*Simulated VSWR of proposed antenna*	*24*
Figure 3.5	*Simulated peak gain of proposed antenna*	*24*
Figure 3.6	*Simulated reflection coefficient of proposed antenna with DE*	*25*
Figure 3.7	*Simulated VSWR of proposed antenna with DE*	*26*
Figure 3.8	*Simulated peak gain of proposed antenna with DE*	*26*
Figure 3.9	*Simulated current distribution of proposed antenna with DE*	*28*
Figure3.10	*Simulated 3D radiation pattern of proposed antenna*	*29*
Figure 4.1	*Design configuration of proposed antenna*	*30*
Figure 4.2	*Simulated reflection coefficient of proposed antenna without DE.*	*31*
Figure 4.3	*Simulated VSWR of proposed antenna without DE*	*32*
Figure 4.4	*Simulated peak gain of proposed antenna without DE*	*32*
Figure 4.5	*Simulated reflection coefficient of proposed antenna with DE*	*33*
Figure 4.6	*Simulated VSWR of proposed antenna with DE*	*34*
Figure 4.7	*Simulated peak gain of proposed antenna with DE*	*34*
Figure 4.8	*Simulated current distribution of proposed antenna with DE*	*35*
Figure 4.9	*Simulated 3D radiation pattern of proposed antenna*	*36*
Figure 5.1	*Geometrical configuration of proposed antenna*	*38*

Figure 5.2 Simulated S-parameter curve of proposed antenna..... 39
Figure 5.3 Simulated VSWR of proposed antenna..... 39
Figure 5.4 Simulated peak gain of proposed antenna..... 39
Figure 5.5 Simulated current distribution of proposed antenna..... 41
Figure 5.6 3D radiation pattern of proposed antenna..... 41
Figure 6.1 Flowchart for fabrication procedure of antenna..... 42
Figure 6.2 Photograph of Aglient E5071C VNA..... 43
Figure 6.3 The Photograph of fabricated proposed antenna..... 43-44
Figure 6.4 The comparison of simulated and measured result..... 44
Figure 6.5 Comparison Simulated and measured radiation pattern..... 45
Figure 6.6 Comparison of simulated and measure gain results..... 45
Figure 6.7 The photograph of proposed antenna..... 46
Figure 6.8 The comparison of simulated and measured result..... 47
Figure 6.9 Comparison Simulated and measured radiation pattern..... 47
Figure6.10 The layout for the simulated proposed antenna using Orcard software 48
Figure6.11 The photograph of fabricated antenna..... 49
Figure6.12 The comparison of simulated and measured result..... 49

LIST OF ABBREVIATIONS

CR	*Crossover*
CST MWS V14.0	*Computer Simulation Microwave Software Version 2014*
DE	*Differential Evolution*
DGS	*Defected Ground Structure*
MPA	*Microstrsip Patch Antenna*
RF	*Radio Frequency*
RFID	*Radio Frequency Identification*
RL	*Return Loss*
UWB	*Ultra wideband*
VNA	*Vector Network Analyzer*
VSWR	*Voltage Standing Wave Ratio*
WiMAX	*Worldwide Interoperability for Microwave Access*
WLAN	*Wireless Local Area Network*

CHAPTER 1
INTRODUCTION

1.1 INTRODUCTION

Numerous chances to support the execution of effectively existing signal transmission and processing systems have been presented due to the outburst in information technology and wireless communications [1]. This led to a strong curiosity to develop novel devices and systems. The most vital component of any wireless communication system is antenna. The antenna can be characterized as a device that is utilized to transmit and receive radio waves. There is an interest for effective and reliable antennas for this new range of wireless systems. These effective and efficient antennas may include patch antennas, parabolic reflectors, folded dipole antennas, and slot antennas. Although each antenna has its own pros and cons but without an adequate design, there will be weak signal detection at the receiver and signal transmitted by the radio frequency (RF) system will be ineffectively transmitted. The newly developed modern integrated circuit technology has led to reduced sizes as well as weight of numerous wireless electronic systems such as cell phones. Low profile antennas are required in various wireless communication systems [2]. These low profile antennas are obstructive to a smaller extent and also, weather rarely affects their performance. Microstrip patch antennas (MPAs) also come under the category of low profile antennas. MPAs have a lot of qualities like light weight, low profile, ease of fabrication, compatibility with integrated circuit technology, and low production cost [3]. These qualities have rapidly increased MPAs popularity, applications and stimulated greater research effort to understand and improve their performance. MPAs have many applications such as spacecraft, high performance aircraft, missiles, and space satellites, where the constraints are weight, size, performance, cost, aerodynamic profile, and ease of installation. There are many other commercial applications like wireless communications and mobile radio which use MPAs and hence, they play a very important role in this era of wireless communication systems [3]. MPAs have been executed in numerous alignments like circular, square, triangular, rectangular, elliptical, and trapezoidal [4]. The most common of them are the rectangular shaped patch antenna due to their ease of fabrication, analysis and effective radiation characteristics particularly low cross polarization.

1.2 MICROSTRIP PATCH ANTENNAS

1.2.1 Background

The antenna is intended to receive or transmits radio waves. It is utilized to couple energy from a guiding structure, for example, transmission line or waveguide into free space and the other way around. In this manner, data can be exchanged between various areas with no mediating structure. MPAs are comprised of radiating element on one side of dielectric substrate and ground on other side of same substrate [5].

The possibility of microstrip radiators goes back to the year 1953 when they were proposed by Deschamps. Quite a long while later, Gutton and Baissinot patented a microstrip based antenna. Despite the publication of idea, very little action in microstrip antenna improvement happened throughout the following 15 years or so aside from some work by Kaloi at the U.S. Naval force Missile Test Range in California. This was halfway because of the absence of good microwave substrates [6]. Likewise, around then more intrigue was centered on stripline circuits as more slender and lower cost contrasting options to waveguide components [7].

The application of microstrip radiators to propose useful antennas only started in the early 1970s when the need for thin conformal antennas were required for missiles and spacecrafts and that led to the rapid development of MPAs [7]. Since then, many papers have been written on the methods of improving and utilizing the advantages of MPAs in spite of its disadvantages [8-10]. MPAs have been one of the most rapidly developing research fields in last twenty years. The MPAs provide wider bandwidth which became foremost area of interest in antennas technology, particularly in the fields of communication systems and wideband radar. Therefore, bandwidth characteristics of these antennas have received significant consideration [9].

1.2.2 Physical Configuration

In its most fundamental shape, a MPA comprises of radiating element i.e. patch on one side of dielectric substrate and ground on opposite side of same substrate as appeared in Figure 1.1. The base surface of dielectric substrate is thin and secured with metallization that is filled in as a ground plane and is normally of copper or gold. MPAs transmit essentially in view of adjoining fields between patch edge and ground plane [10].

For effective antenna performance, a thick dielectric substrate having a low dielectric constant is preferable as it gives better performance, wider bandwidth and better radiation. For such antenna characteristics, proposed antenna designs are large. To design smaller size MPAs higher dielectric constants is utilized which in return results in narrow bandwidth with low efficiency, thus antenna dimensions or performance have to be compromised [2,10].

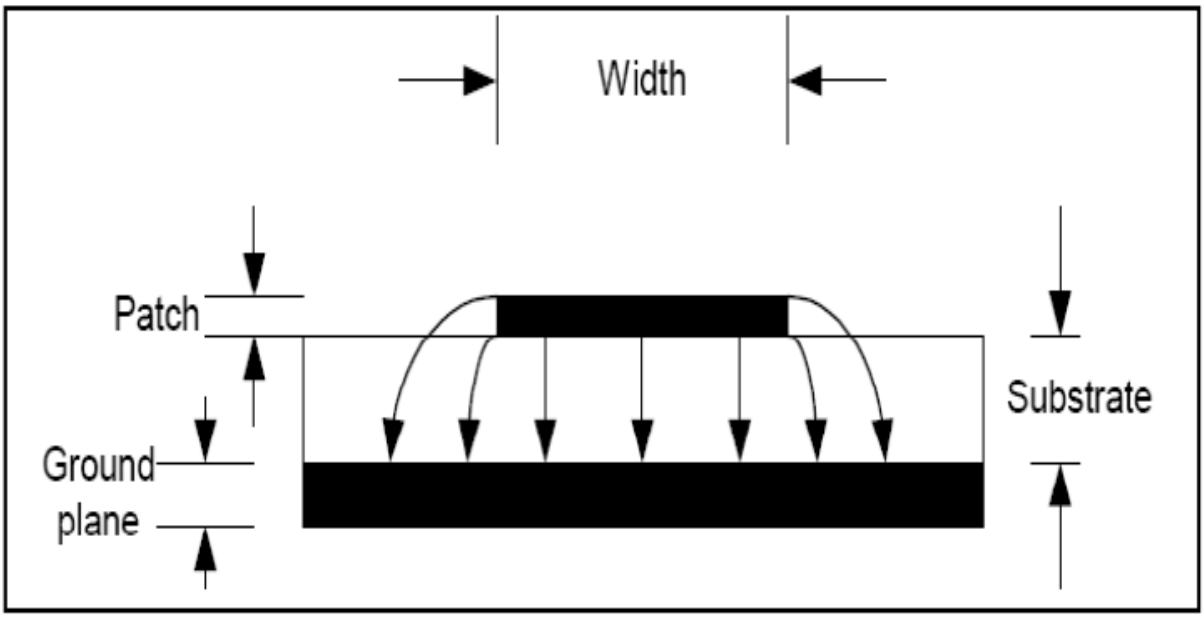

Figure 1.1 Cross-Sectional View of a MPA [7].

The patch is typically made of conducting material and can take any conceivable shape as shown in Figure1.2.

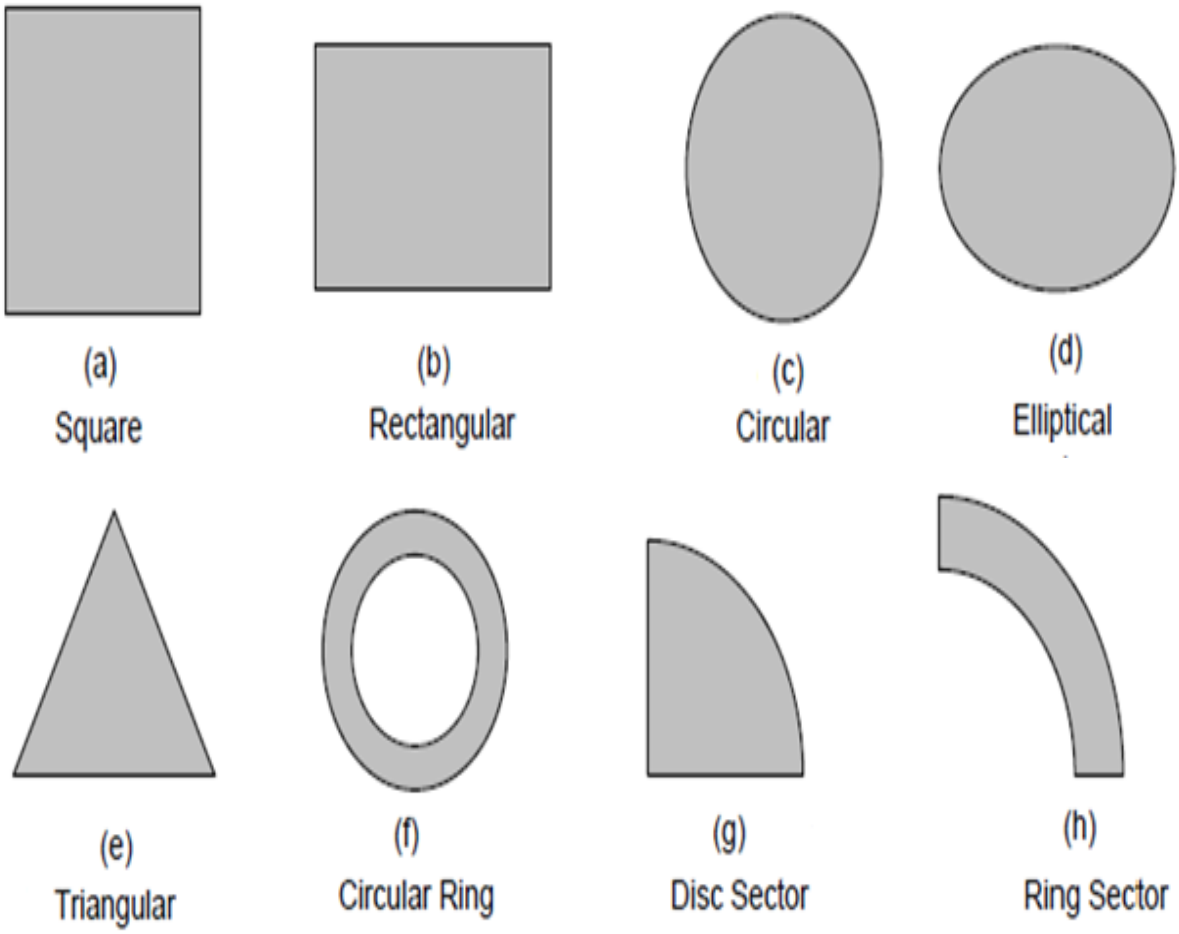

Figure 1.2 Representative Shapes of MPAs [7].

The rectangular shaped antenna is the most well-known sort of MPAs as a result of its ease in the analysis, fabrication, and its effective radiation qualities particularly low cross polarization radiation. This is made of rectangular shape radiating patch with configurations width (W), length (L), thickness of substrate (h) and dielectric constant (r) as represented in Figure 1.3 [11, 12].

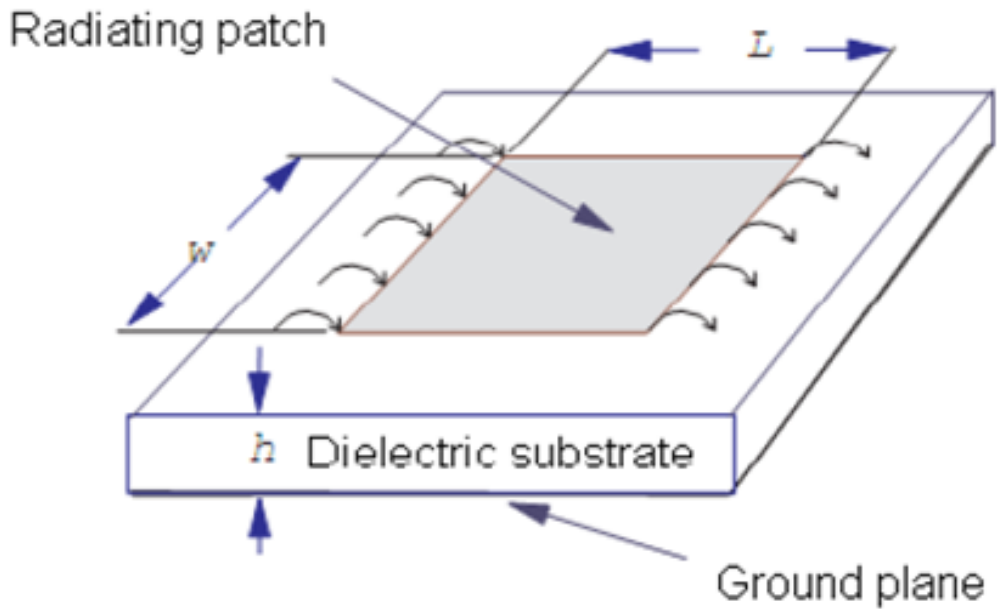

Figure 1.3 Structure of Rectangular MPA.

1.3 ANTENNA PROPERTIES

1.3.1 Gain

This is the amount which depicts the ability of antenna to concentrate power in a particular direction. In many cases, transmission is required between a transmitter and just a single receiving station [5-7]. Power is in this manner transmitted in particular direction since it is valuable just toward that path. Transmitting and receiving antennas ought to have little power losses and ought to be productive as radiators and receptors. Gain is expressed in dB and is characterized as antenna directivity times a component representing the radiation efficiency and its expression is as per the following;

$$G = \eta \times D \qquad \text{Equation (1.1)}$$

Where G represents gain of antenna, η efficiency of antenna and D directivity of antenna.

1.3.2 Voltage Standing Wave Ratio (VSWR)

VSWR is defined as measurement of impedance mismatch between feed point and antenna. The effective power transmission takes place when input impedance of antenna and feeding

source matches [7]. Thus higher the value of VSWR more is the mismatch of input impedance. The ideal possible value of VSWR is unity.

$$VSWR = \frac{1+|\Gamma|}{1-|\Gamma|} \qquad \text{Equation (1.2)}$$

Where, Γ is the reflection coefficient.

1.3.3 Return Loss (RL)

RL is a proportion of power transferred to source to power reflected back. To acquire ideal matching between feeding system and antenna; $\Gamma = 0$ and RL = - infinity, in this case no power is reflected back. RL is given as;

$$RL = -20\log|r| \qquad \text{Equation (1.3)}$$

1.4 ADVANTAGES AND DISADVANTAGES OF MICROSTRIP PATCH ANTENNAS

In recent years, the utilization of MPA in wireless communication has expanded fundamentally. This is because of their low-profile which is the most attractive feature of MPA [10]. However, along with this feature it posses many other advantages and disadvantages also as discussed in next section.

1.4.1 Advantages of MPAs

- Compact size with light weight.
- Low fabrication cost, consequently large scale manufacturing.
- Linear and circular polarization is both supported.
- Capability of multi band frequency operations.
- Simultaneous fabrication of feedline and matching network is possible.

1.4.2 Disadvantages of MPAs

- Narrow bandwidth and low gain with low effectiveness.
- Surface wave excitation and superfluous radiation from feedline and junctions.
- Low power dealing capability.
- Complex feeding structures requiring superior clusters.

1.5 MICROSTRIP PATCH ANTENNAS FEED TECHNIQUES

Various feeding strategies are used for feeding the antenna. They are classified as: MPAs can be contacting and non-contacting techniques. Contacting feed strategy is one in which radiating element of antenna is directly fed by a connecting component such microstrip line. Non-contacting strategy is one in which electromagnetic coupling is utilized to exchange

power between feeding source and radiating element. The most well known contacting feed procedures utilized are microstrip line feed and coaxial probe feed, while the most famous non-contacting feed methods are aperture coupling feed and proximity coupling feed [7]. The feeding technique that we are utilizing as a part of our model is microstrip feed line.

1.5.1 Microstrip Line Feed Technique

This feed strategy utilize conducting strip that is specifically associated with the edge of microstrip patch as appeared in Figure 1.4. The conducting strip and patch both can be created on a similar substrate at same time which results in a planar structure [7]. The width of a conducting strip is smaller than that of patch. This strategy gives a simple and ease to fabrication, modeling and particularly in the impedance matching.

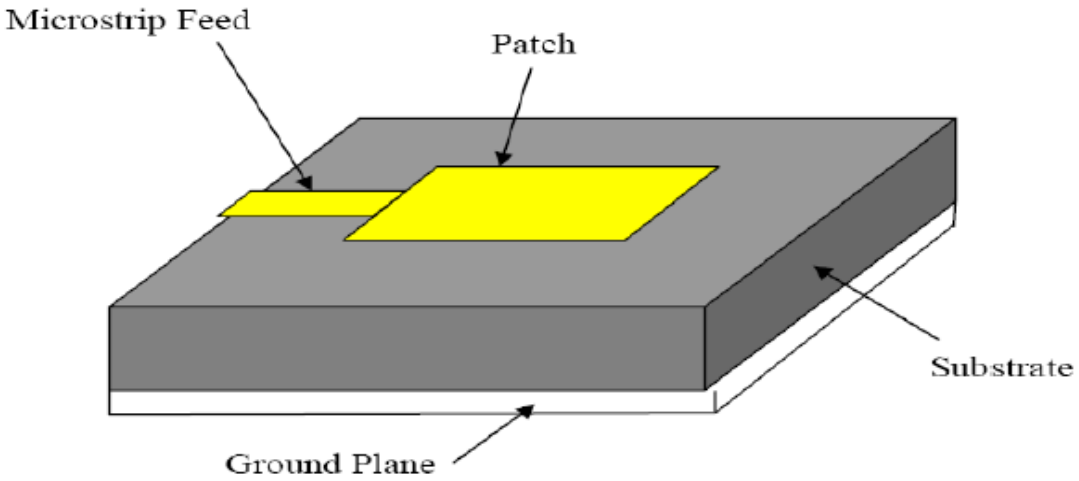

Figure1.4 Microstrip Line Feed Technique [7].

1.5.2 Coaxial Probe Feed Technique

In this feed technique inner coaxial conductor is soldered to radiating element i.e. patch by passing through substrate whereas outer coaxial conductor is attached to ground plane.

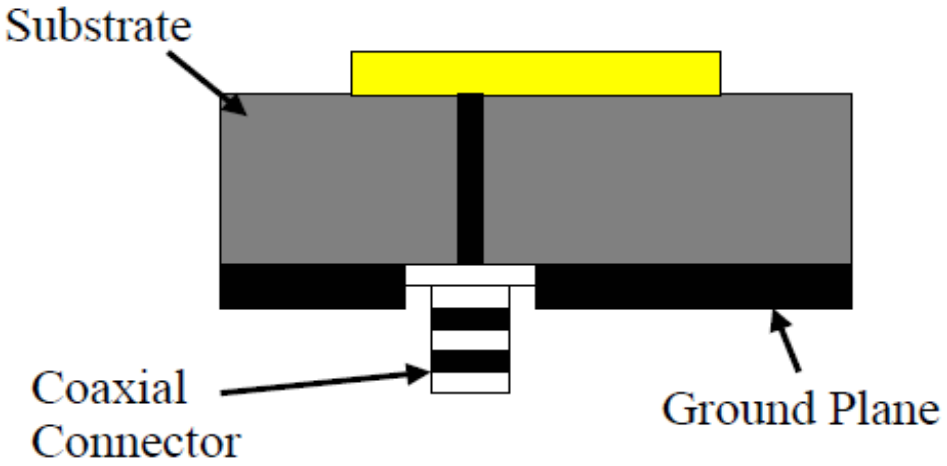

Figure1.5 Coaxial Probe Feed Technique [7].

1.5.3 Aperture-Coupled Feed Technique

In this feed technique ground plane separates radiating patch and microstrip feedline. A slot or a coupling aperture centered under patch in ground helps to make coupling between patch and feedline [7].

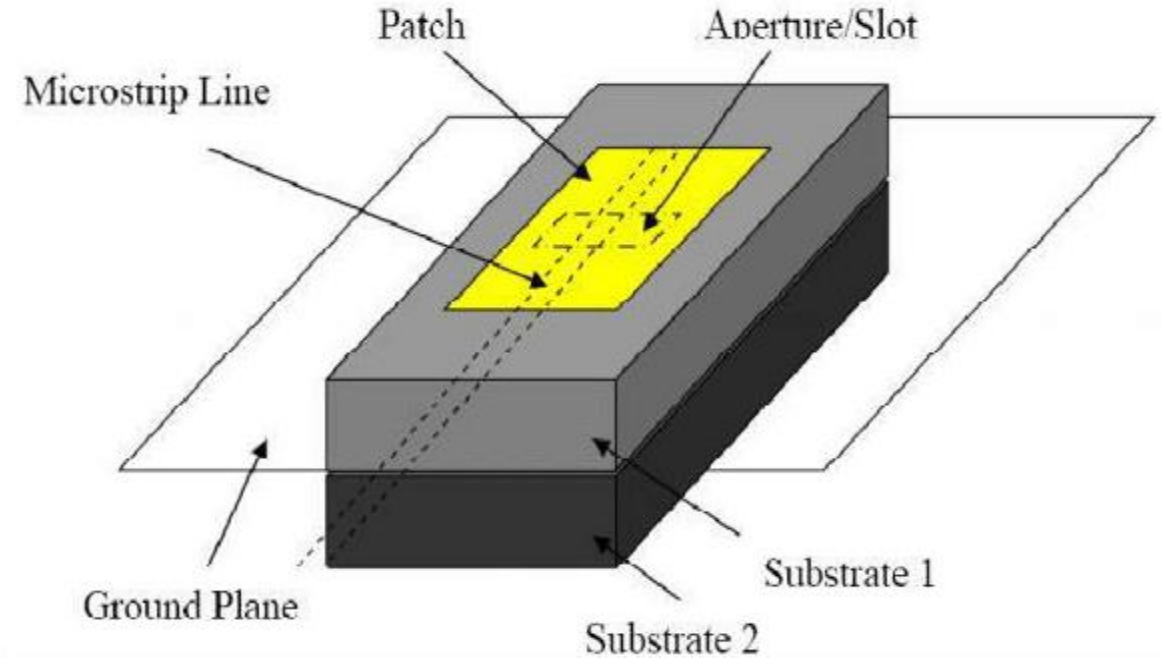

Figure1.6 Aperture-Coupled Feed Technique [7].

1.5.4 Proximity-Coupled Feed Technique

Another name for this type of feed technique is electromagnetic coupling scheme. The structure of this feed is such that a feed line is present between two dielectric substrates with patch on top.

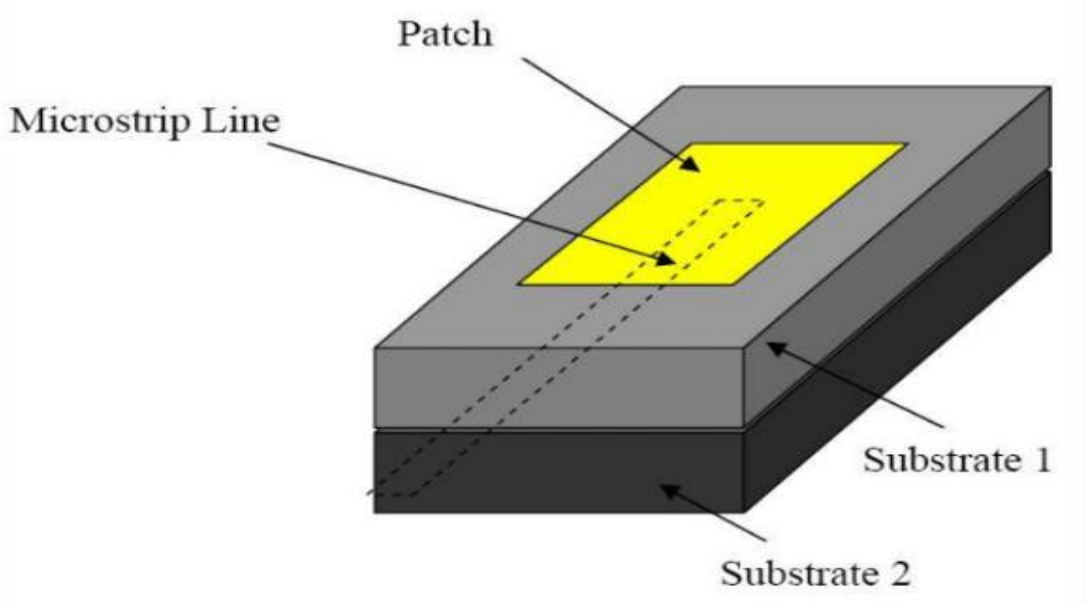

Figure1.7 Proximity-Coupled Feed Technique [7].

Table 1.1 illustrates the characteristics of various feed techniques discussed in above section.

Characteristics	Coaxial probe feed	Microstrip line feed	Aperture coupled feed	Proximity coupled feed
Configuration	Non planar	Coplanar	Planar	Planar
Ease of fabrication	Soldering and drilling needed	Easy	Alignment required	Alignment required
Spurious feed radiation	More	More	Less	Minimum
Reliability	Poor due to soldering	Better	Good	Good
Impedance matching	Easy	Easy	Easy	Easy
Polarization purity	Poor	Poor	Poor	Poor
Bandwidth	2-5%	2-5%	About 15%	About 13%

Table 1.1 Comparison of different Feed Techniques.

1.6 APPLICATIONS OF MICROSTRIP PATCH ANTENNAS

The utilization of the MPAs is spreading largely in both business and non-business view points because of low cost substrate material and simplicity of fabrication, with the most applications being on mobile communication [12]. MPAs are generally relevant where lightweight, low profile, and low cost conformal structures are required.

1.6.1 Mobile and Satellite Communication Application

MPAs are mostly utilized as a part of mobile communication. On account of satellite communication, circularly polarized radiation patterns are typically utilized and can be acknowledged by square or circular radiating patch with multiple feed points.

1.6.2 Global Positioning System Application

MPAs are utilized for global positioning system because of its simplicity in coordination of a low noise amplifier on substrate used for feeding hardware. These antennas are normally circularly polarized.

1.6.3 Radio Frequency Identification (RFID)

RFID systems comprise of a tag or transponder and transceiver or reader RFID and are utilized in various areas like mobile communication, logistics, transportation and medical field [5]. The frequency between 30Hz and 5.8 GHz are utilized for its applications.

1.6.4 Worldwide Interoperability for Microwave Access (WiMAX)

MPAs are utilized for WiMAX as they meet the IEEE 802.16 standard.

1.6.5 Radar Application

For detecting moving targets such as individuals and vehicles radar are used [6]. A low profile and light weight antenna subsystem demand make MPAs most preferable choice.

1.7 DIFFERENTIAL EVOLUTION ALGORITHM

Differential Evolution (DE**)** Algorithm is a strategy that optimizes a problem by utilizing iterative method to improve a candidate solution to a given measure of quality [13]. Such techniques are generally referred to as metaheuristic as they make few or no assumptions about the issue being and would be able to search vast spaces of candidate solutions.

The utilization of DE is in multidimensional real-valued functions, yet they do not use gradient of problem to be optimized. Thus DE does not require the optimization problem to be differentiable as required in classic optimization techniques. This optimization technique improve the results by maintain a population of candidates solutions and developing new candidate solutions by combination of all presented ones according to its simple formulae and then considering the candidate solution with best score or fitness value [13]. Thus the optimization technique is considered as a black box that gives simple measure of quality giving a candidate solution and therefore gradient is not required.

1.7.1 History

DE was grown out of Ken Price's attempts to tackle the Chebychev Polynomial fitting problem that had been presented to him by Rainer Storn [13]. With this Ken came up with the idea of utilizing vector differences for perturbing vector populations. After this creative idea many discussion between Ken and Rainer took place and with endless ruminations and computer simulation, both yielded many considerable improvements that resulted in making DE a versatile and robust tool for today’s research work.

1.7.2 Overview

DE is a basic population based, stochastic function minimize which become very popular in recent years. DE managed to finish 3rd at the First International Contest on Evolutionary Computation (1stICEO) which was held in Nagoya, may 1996. DE was considered as one of the best genetic type algorithm for solving real-value test functions [15]. The fundamental idea of DE is that it generates trial parameter vectors for solving the problem. Figure 1.8 shows the procedure for DE in sequential manner.

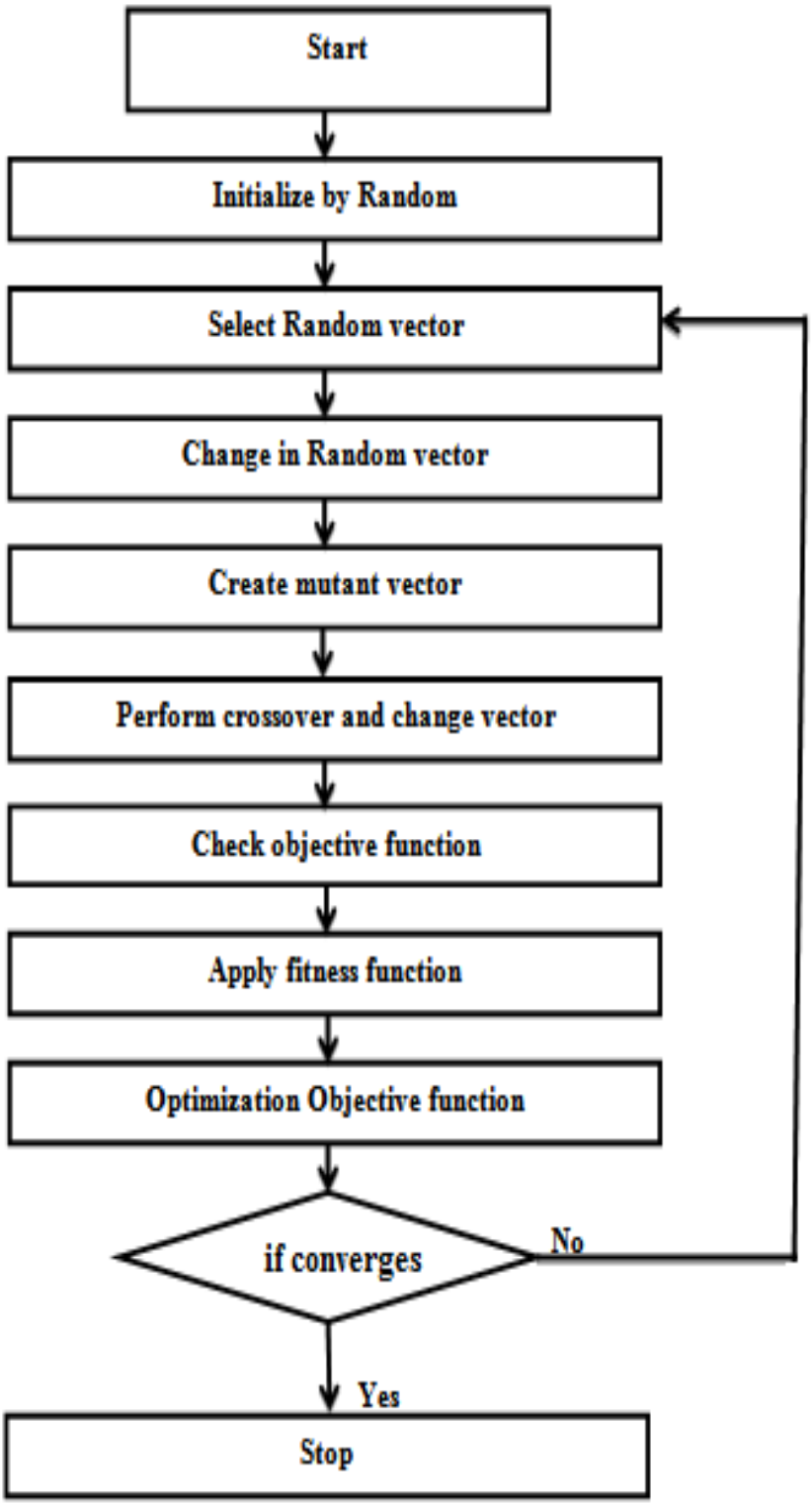

Figure 1.8 Flowchart of DE Algorithm [13].

1.7.3 Example of DE Algorithm

Objective Function:

Minimize f (x) = x1 + x2 + x3

Population Size NP = 6 (user defined) D = 3

The initial population is chosen randomly from 0 to 1 for 3 decision variables. Table 1.2 represents the population along with the objective function [13]. The first individual i.e. individual 1 is considered as a target vector.

	Individual 1	Individual 2	Individual 3	Individual 4	Individual 5	Individual 6
X1	0.68	0.92	0.22	0.12	0.40	0.94
X2	0.89	0.92	0.14	0.09	0.81	0.63
X3	0.04	0.33	0.40	0.05	0.83	0.13
f(x)	1.61	2.17	0.76	0.26	2.04	1.70

Table 1.2 The intial population along with the objective function.

The next step includes the generation of nosiy random vector. For this three individuals i.e. individual 2,4 and 6 are selected randomly from the intital population size. This proceed with weighted difference between two individuals (2 and 4), adding to third randomly chosen individual (6). The scaling factor F is user defined and ranges from 0.5 to 1.0 and it represents the probability of child vector inherits parametric values from generated noisy random vector. Table 1.3 illustrates the calculation of weighted difference vector. Table 1.4 represents the calculation for generating noisy random vector.

	Individual 2	Individual 4	Difference Vector		Weighted difference vector
X1	0.98	0.12	= 0.80		= 0.64
X2	0.92	0.09	= 0.83	* F (F = 0.80)	= 0.66
X3	0.33	0.05	= 0.28		= 0.22

Table 1.3 Calculation of Weighted Difference Vector [13].

Further for generating the trial vector noisy random vector does crossover (CR) with target vector. CR is also user defined constant ranging from 0.5 to 1.0.

	Weighted difference vector		Individual 6	Noisy random vector
X1	= 0.64		0.94	= 1.58
X2	= 0.66	+	0.63	= 1.29
X3	= 0.22		0.13	= 0.35

Table 1.4 Calculation of Noisy Random Vector [13].

This procedure is done by generating random numbers equal to the dimension of problem for each dimension: if random number > CR; copy the target vector value, else copy the value from noisy random vector. In this case, the value of CR is considered as 0.50. Table 1.5 represents the generation of trial vector.

	Target vector		Noisy random vector	Trial vector
X1	= 0.64		1.58	= 1.59
X2	= 0.66	CR = 0.50	1.29	= 0.89
X3	= 0.22		0.35	= 0.04
F (x)	1.61		3.22	2.51

Table 1.5 Generation of the trial vector [13].

The objective function of trial vector and target vector is compared and one with the minimal estimation of two considered for next generation as Individual 1. Further for generating individual 2 for next generation, the second member of initial population is considered as target vector and above procedures is repeated. Table 1.6 represents the new population for next generation.

	Individual 1	Individual 2	Individual 3	Individual 4	Individual 5	Individual 6
X1	0.68					
X2	0.89					
X3	0.04					
f(x)	1.61					

Table 1.6 New population for next generation [13].

This procedure is repeated NP times for completing one generation which fills the new populations set. Once the end criteria is met algorithm finishes.

1.8 PROBLEM STATEMENT

The issue articulation of proposed examine work is to set up the best design of MPAs with dual-frequency behavior utilizing novel plans of radiating element (patches) and ground structures. We will probably contemplate dual-frequency and multi-frequency MPAs appropriate for wireless applications and to give a structure for tackling different outline issues of MPAs to develop new techniques for obtaining multiband operation. For getting the profound knowledge of antennas suitable for various applications [16], different antenna structures have been considered which are discussed in next chapter. The designed antennas are being fed using Microstrip feeding technique. Also antenna miniaturing is required to avoid large size of antennas for operating at lower frequencies with more return loss and wider bandwidth [16]. Earlier, designing of MPAs included numerical and analytical methods. On the other hand, the numerical methods are unable to design a feasible practical antenna in a decent amount of time. From these, the analytical methods are the most useful in providing a better instinctive clarification of the MPAs operation and for practical designs. On the other hand, the numerical methods are unable to design a feasible practical antenna in a decent amount of time. Also, these methods require detailed background knowledge and the calculations are time consuming those need really high-priced software packages. A simple and effective design is preferred because of the ever-increasing need for MPAs [17]. Lately, numerous improved methods in MPA designing have been reported, these include the introduction of artificial intelligence methods like Particle Swarm Optimization, Artificial

Neural Network and Genetic algorithm. However, there are many challenges posed by these softwares as they can be challenging to learn because of their complicated design and hence, these have become quite infamous among various engineers. So, there is a need to introduce a new technique which uses less of the computer memory and performs the work for effective designing. Various other techniques have been introduced using numerous artificial intelligence techniques [18]. Also, many patch designs and various design methodologies have been verified to provide better radiation characteristics and gain. This report demonstrates DE algorithm to develop an optimal parametric design procedure in the process of modeling a rectangular MPAs.

1.9 RESEARCH OBJECTIVES & JUSTIFICATION OF THE STUDY

- Design of dual-band rectangular MPA using DE algorithm for diverse wireless application.
  - Implementation of DE algorithm on proposed antenna.
  - Reducing computation complexity by using DE algorithm
  - Fabrication and testing of proposed antenna.
- Design and optimization of modified T-shape MPA using DE algorithm for X and Ku band application.
  - Implementation of DE algorithm on proposed antenna.
  - For easy control and implementation of antenna parameters.
  - Fabrication and testing of proposed antenna.
- Design of hand-fan shaped MPA U-slot defected ground structure (DGS) for L-band and S-band applications.
  - Designing and simulation of proposed antenna.
  - Improvement in antenna characteristics such as reflection coefficient, bandwidth, gain and radiation pattern.
  - Fabrication and testing of proposed antenna.
  - Effect of U-slot DGS and hand-fan shaped patch on proposed antenna
- To compare the simulated and measured result for all the proposed designs.

To accomplish the above stated research objectives and to outline the potential adequacy of proposed MPAs, a collection of broadened issues with different encounters have been considered and solved. These issues are as follows:

- Effect of DGS and slots etched in radiating element and implementation of DE algorithm on proposed antenna (Chapter 3).
- Effect of Inset-fed line feeding technique, slots etched in patch and ground plane and implementation of DE algorithm for optimizing antenna parameters of proposed antenna (Chapter 4).
- Effect of U-slot DGS and hand-fan shaped patch on proposed antenna (Chapter 5).

1.10 ORGANIZATION OF THESIS

Chapter 1 covers the problem background together with the goals of the research. The literature review is expounded in Chapter 2. This section presents MPAs concept, and pertinent areas of use which likewise incorporates the strategy for differential evolution algorithm. Chapter 3 deals with designing and optimization of DE algorithm based dual-band rectangular MPA for diverse wireless application which incorporates analysis and formulation of the project results about depicting the plan system for this type of antenna. Chapter 4 analyses and talks about the simulation and experimental results of modified t-shape MPA using DE algorithm for x and ku band applications. Chapter 5 introduces the outline strategy for designing hand-fan shaped MPA with U-slot DGS for L-band and S-band applications which incorporates analysis and formulation of the project results about depicting the plan system of the rectangular MPA .Chapter 6 deals with fabrication and testing of the proposed antennas that were discussed in Chapter 3, 4 and 5. Chapter 7 finishes up the work performed in this report with recommendations for future work. Lastly, publications and references are incorporated toward the finish of the report.

CHAPTER 2
LITERATURE SURVEY

Singh I. *et al.* in [10] investigated MPA or incredible advancement in recent years. MPAs are more interested with better prospects as compared to other conventional antennas. They are lighter in weight, low profile, smaller in measurement and simple in manufacturing. In addition, MPAs can give dual and circular polarizations, multi band frequency operations, wider bandwidth, feedline adaptability, beam scanning omnidirectional designing.

Saeed R. *et al.* in [12] theoretically examined square fed aperture coupled MPA which is applicable for wireless applications with resonant frequency at 2.4 GHz with 80 MHz bandwidth. The radiating patch focuses on slots for maximum coupling and patch in respect to slots in H-plane has little impact, while patch in respect to slots in E-plane diminishes the coupling level.

Zhang H. *et al.* in [14] designed a MIMO antenna to resonate at 2.65 GHz with 3 equilateral triangle MPA components. The SNR and interference rejection of MIMO system is enhanced with high gain for every antenna system due to wide beam qualities of triangular MPA. This study reveals that mutual coupling and relation between each mach of antenna ports helps in accomplishing great antenna polarization and directivity.

Kaur J. in [15] proposed a triple-band antenna for wireless applications. This antenna design covers multiple frequencies ranging from 2.35-2.86, 3.0-4.3 and 5.64-6.85 GHz with total bandwidth of 510 MHz, 1.3 MHz and 1.21 MHz respectively. To accomplish this result a strip was coupled on right side of O-shaped patch and ground plane in modified to L-shape with two unequal slots. The frequency range covered in proposed work was applicable for wireless applications.

Shambavi K. in [16] presented a probe fed MPA with identical dual square antenna stacked on top other with an air gap for enhancing gain and bandwidth. An air gap height is so considered that maximum gain and bandwidth was accomplished. This proposed antenna can be utilized in field of wireless application with resonant frequency at 2.4 GHz.

Dheyab A. *et al.* in [17] presented a paper to overcome problem of MPA of low efficiency, narrow bandwidth and surface wave losses by using different thickness of dielectric substrate such 4 mm, 6 mm and 8 mm. At 6 mm the simulated rectangular patch antenna gave bandwidth of 200 MHz with operating frequency at 2.4 GHz. The proposed antenna configurations were simulated and verified using Microwave office 2000 software. A good impedance matching of 50 ohm at feeding point was obtained by trial and error method.

Liu W.C. *et al.* in [18] investigated new microstrip fed planar monopole antenna for triple-frequency. This antenna has a rectangular patch with L-shaped inverted dual strips fed by cross shaped stripline and DGS was utilized in this antenna design for accomplishing multiple resonant frequencies and enhanced bandwidth. This antenna has overall compact size of 20x30 mm^2 and with 2.14-2.52 GHz, 2.82-3.74 GHz and 5.15-6.02 GHz resonant frequencies. These frequencies have application in the field of wireless communication such as WLAN and WiMAX.

Agarwal N. *et al.* in [19] presented a design and manufacture procedure of rectangular MPA working at 2.0 GHz. Extensive emphases are put on designing of rectangular MPA and antenna results obtained through IE3D software. The proposed probe fed rectangular MPA operates at 2.0 GHz frequency.

Kaur J. *et al.* in [20] designed monopole antenna with multistrip feb by cross shaped stripline, having one vertical and two horizontal strips for WLAN, ISM, IMT, Bluetooth and WiMAX. The DGS is utilized in this proposed antenna for obtaining dual band operation with considerable bandwidth applicable for several communication standards at dual operating band.

Karli R. *et al.* in [21] introduced a simple MPA at 2.45 and 5.8 GHz operating frequencies that are reserved for RFID and WLAN applications. For considered antenna design, simulation and antenna characterization was performed using CST software. The measured and simulated results were compared. The proposed antenna has simple and compact structure, resulting in good impedance matching with wider bandwidth and suitable gain.

Yassen M.T. *et al.* in [25] designed offset microstrip fed two patch slotted antenna with resonant frequency at 2.4 and 5.2 GHz applicable for WLAN applications. The primary patch

has rectangular shape where as other has inverted L shape along with a stub protruding from it. The proposed antenna has dual band characteristics with 2.3996-2.6309 GHz and 5.1335-5.8065 GHz bandwidth having -10 dB RL.

Anguera J. *et al.* in [27] presented a work to give a review of development that wireless handheld technology has encountered in the most recent years. In this sense, a depiction of development of wireless handheld gadgets, challenges in the present smartphones, and handset features were surveyed. In this work advancement in antenna technology for wireless handheld or portable gadgets were discussed.

Singh R. *et al.* in [38] proposed a compact size MPA for wideband applications. This antenna accomplishes wide impedance bandwidth by cutting the rectangular shape radiating patch into the defected shape. The ground and the patch were on the same side of the material (FR-4).The antenna results were achieved by CST software. The proposed antenna resonates at three frequencies 11.2, 12.5 and 14.3 GHz from 10.5 to 16.4 GHz, which is appropriate for X and Ku band applications.

Arunachalam V. in [13] clarified in detail the working of DE algorithm calculation. It likewise gave documentation to the utilization of Differential Evolution PC program to take care of user-defined optimization issues. The PC program was composed in C language for Windows. The book additionally exhibits how to alter the program utilizing a case optimization issue.

Zhong M. *et al.* in [29] presented a work to optimize a spherical luneberg lens (SLL) using differential evolution algorithm. Specifically, unique consideration is given to the ideal gain of lens antenna. In this work a five-layered SLL was optimized using DE algorithm and was verified by spherical vector wave function expansions (SWE). The calculated radiation characteristics show good agreement with simulated results by commercial software.

Chowdhury A. *et al.* in [31] presented a numerical strategy, called Fitness Adaptive Differential Evolution (FiADE) for enhancing certain pre-defined antenna setup to accomplish best radiation characteristics. DE propelled by normal marvel theory of advancement of life on earth, utilizes comparable computational steps as by any other EA. F and CR probability are two essential control parameter of DE.

Deb A. *et al.* in [32] designed a probe-fed MPA utilizing DE algorithm. The cavity model was analyzed for fitness function. The optimized results obtained by implementation of DE were compared with other algorithms such as GS and PSO.

Tanabe R. *et al*. in [33] proposed a parameter adaptation strategy that utilizes verifiable memory to control parameters to manage future control parameter esteems for DE. This stratergy was assessed by correlation on 28 issues from CEC2013 bench set, and additionally CEC2005 benchmarks and set of 13 classical benchmark problems. The experimental results demonstrated that DE utilizing success history based parameter adaptation strategy was competitive with state-of-the-art DE algorithms.

Zhao W.J. *et al.* in [34] presented a technique to determine parameters of equivalent dipoles by minimizing objective function. The local optimization algorithms problem was limited by exhibiting local minima of objective function. The DE algorithm was found to overcome these limitations and experimental data was used to verify proposed approach.

Deb A. *et al.* in [35] presented a design of aperture coupled MPA using DE. The optimization algorithm was utilized to decide dimensions and feed line position to obtain better matching for a given operating frequency and substrate. For designing aperture coupled MPA using DE, fitness function was assessed by method of moments (MOM) system executed through IE3D. Antenna optimized using code for GA and PSO were also done and results were compared with that obtained by DE.

CHAPTER-3

DESIGN OF DUAL-BAND RECTANGULAR MICROSTRIP PATCH ANTENNA USING DIFFERENTIAL ALGORITHM FOR DIVERSE WIRELESS APPLICATION

The proposed antenna is presented and discussed for complete geometrical technique. The fabrication and measurement of proposed antenna designed using optimized parameters found out using DE to verify the simulation results in the succeeding sections.

3.1 INTRODUCTION

In this work, the main focus is on designing the microstrip-line fed dual band rectangular patch antenna with appreciable gain and bandwidth [19-22]. The antenna performance can be improved by optimizing various geometrical parameters of antenna [23-27]. Here, instead of using hit and trial methods for antenna parameter optimization, we prefer to use DE algorithm. DE is carried out in four steps viz. Initialization, Mutation, Crossover and Selection. Mutation and Crossover are user defined parameters and have a noteworthy influence on the performance of algorithm [29, 30]. Next section briefly describes the steps for DE.

STEP 1: For the target vector an initial population is being defined as ($X_i^l < X_{i,j}$ rand(0,1) < X_i^u) where $X_{i,j}$ are randomly selected vectors. Different parameters of antenna design are considered for target vector which are to be optimized. A lower limit and a upper limit is assigned to each parameter.

STEP 2: On the interval (X_i^l, X^u_i) the initial parameter values are consistently selected in a random manner where X_i^l and X^u_i reveal the lower and upper limit of randomly selected vectors respectively.

STEP 3: Parameter vectors are selected randomly for each target vector.

STEP 4: To form a donor vector, the weighted difference of two parameters are added to third vector and it is referred as a mutation vector.

$$V_{k,n}(t+1) = X_{m,n}(t) + F * ((X_{i,n}(t) - X_{j,n}(t)) \qquad \text{Equation (3.1)}$$

where, $V_{k,n}(t+1)$ is the mutation vector or donor vector and $X_{m,n}(t)$, $X_{i,n}(t)$ and $X_{j,n}(t)$ are randomly chosen integers. Here F is known as a scaling factor that scales the difference of two parameter vectors and adds it to the third one. The range of scaling factor is from 0 to 2.

STEP 5: To obtain the trail vector donor vector does CR with the target vector. The CR is performed for generating the trial vector. CR is a user defined probability parameters ranging from 0 to 1. The parametric values for trial vector are being inherited from the mutant vector.

$$T_{k,n}(t+1) = V_{k,n}(t+1) \text{ if rand } (0,1) < CR$$

$$= X_{k,n}(t) \text{ otherwise} \qquad \text{Equation (3.2)}$$

Where $T_{k,n}(t+1)$ represents trail vector or a new vector.

STEP 6: For the next generation, comparison of the trial vector and corresponding target vector is carried out. With the best fitness value one out of both is selected for next generation. Figure 3.1 illustrates the flowchart of DE algorithm which describes the workflow in a sequential manner to be executed for the implementation of the said algorithm.

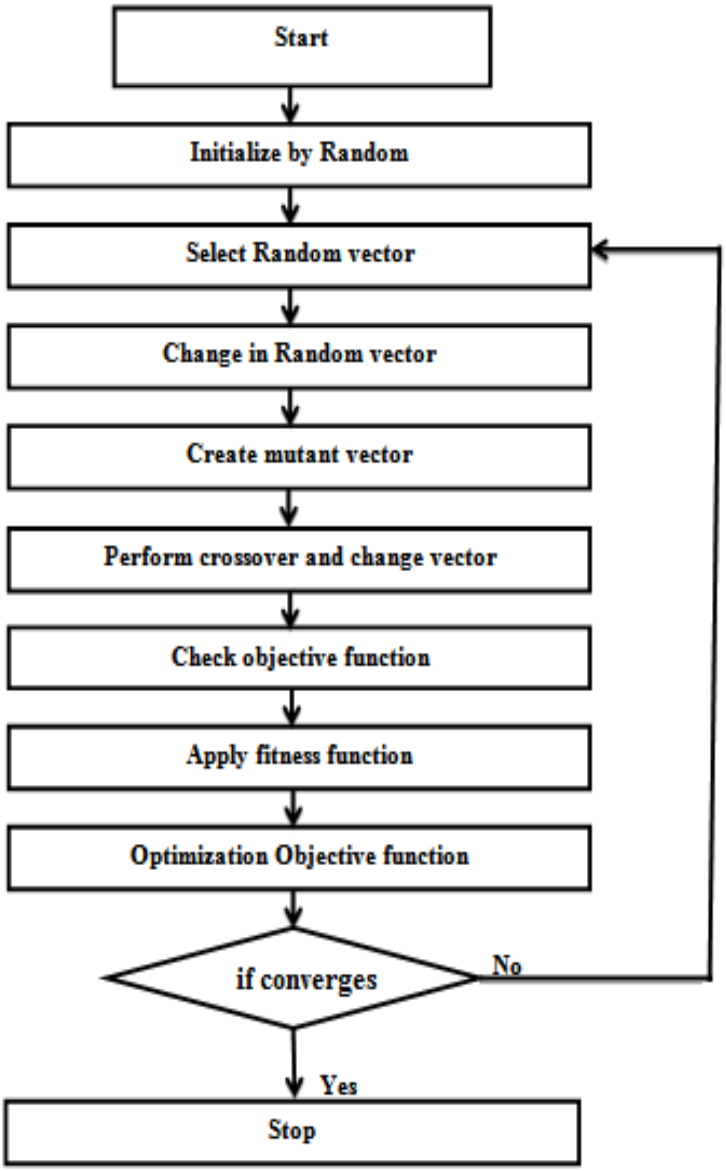

Figure 3.1 Flowchart of differential evolution algorithm [29].

3.2 ANTENNA DESIGN AND SIMULATION RESULTS WITH AND WITHOUT DE

Figure 3.2 (a-b) represents the configuration for proposed antenna covering dual frequency band. Figure 3.2 (a) and 3.2 (b) represents the overall geometry for top and bottom view of microstrip-line fed rectangular patch antenna. This antenna has been drafted on insulating dielectric substrate of low loss thin sheet. On the opposite sides of an inexpensive material FR4 the radiating patch and ground are etched, considering a dielectric constant of 4.4, substrate thickness of 1.57 mm and loss tangent of 0.0025. The slots with various dimensions are etched on both the non-radiating edges of rectangular patch. The ground plane is also been reduced and modified with a slot in it referred to as DGS. These slots are responsible for impedance matching, enhancing bandwidth and for improving antenna radiation characteristics. The microstrip feedline is fabricated on the upper side of the substrate to feed the radiator, which touches the patch on one end, and the other end of the feedline touches the end point of the substrate along its width. On whole dimensions of antenna is L x W with the size of the ground, radiating element and feedline taken to be as L_g x W_g , L_p x W_p and L_f x W_f respectively. Further various slots etched on the patch are represented as S_1, S_2, S_3 and S_4. The slot in ground has its dimension as L_{gs} x W_{gs}. For good impedance matching, the patch is being fed by 50-ohm transmission line. Table 3.1 represents the design specifications of various elements for proposed antenna.

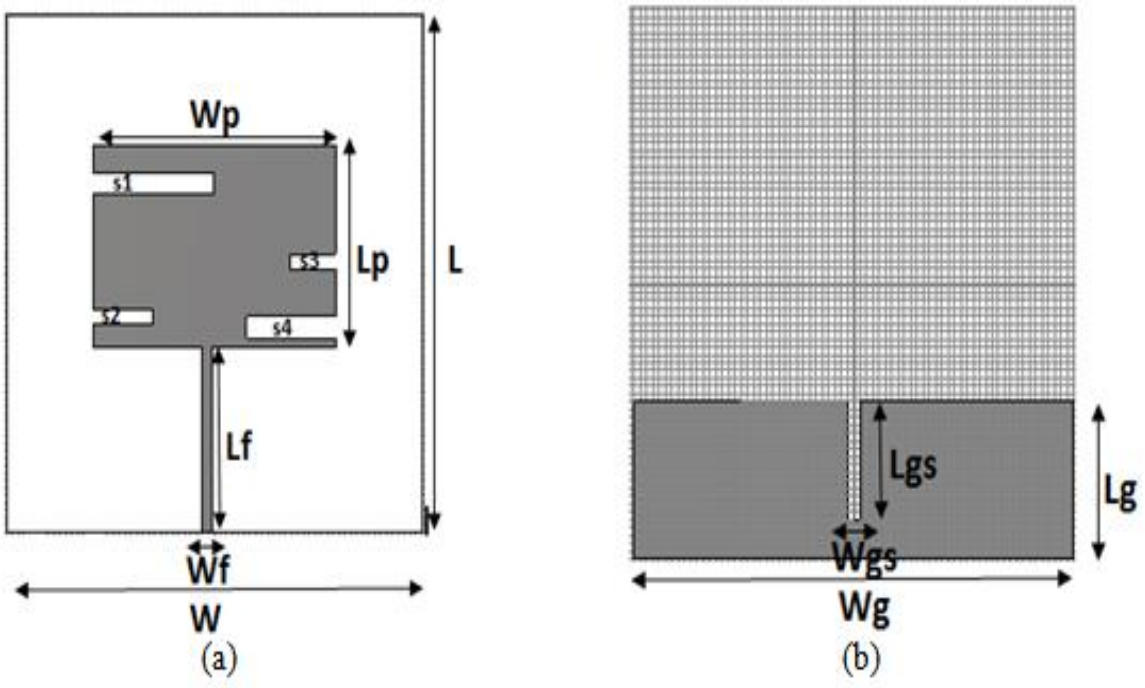

Figure 3.2 Geometrical configuration of proposed antenna (a) Top view (b) Bottom view.

Elements	Dimensions (mm)
Substrate	$L = 70$; $W = 70$
Patch	$L_p = 7.5$; $W_p = 40.70$
Ground plane	$L_g = 20$; $W_g = 70$
Slots	$S_1 = S_3 = 2 \times 20.35$; $S_2 = S_4 = 2 \times 19$ $L_{gs} = 15$; $W_{gs} = 1$

Table 3.1 Specifications of proposed antenna.

3.2.1 Simulation Results for S-Parameter, VSWR and Gain without DE

The proposed antenna configuration is investigated using CST MWS V14.0 which is three dimensional electromagnetic software that is commercially available and it is based on finite integration technique. The performance of antenna can be evaluated using reflection coefficient as well as VSWR.

Figure 3.3 shows simulated return loss of proposed antenna resonating at several frequency bands without using optimization algorithm. This plot of reflection coefficient for proposed antenna clearly indicates that it resonates at 2.49 GHz, 5.62 GHz and 6.27 GHz. The proposed antenna covers an impedance bandwidth of 110 MHz (2.43 – 2.54 GHz), and 480 MHz (5.40 - 5.88 GHz) and 470 MHz (6.00 - 6.47 GHz) for the three respective resonating frequencies.

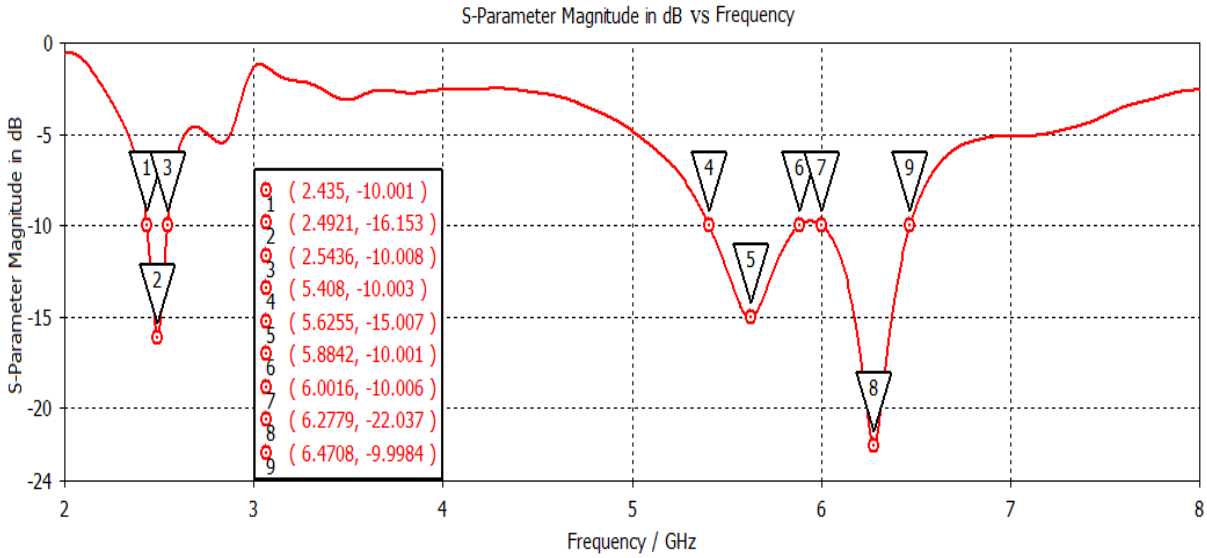

Figure 3.3 Simulated reflection coefficient of proposed antenna.

The simulated VSWR of proposed antenna is shown in Figure 3.4. The VSWR value was found as 1.37, 1.43 and 1.63, which is less than 2, the impedance transformation ratios were 1:1.3, 1:1.43 and 1:1.63 for the three operating frequency bands at 2.49 GHz, 5.62 GHz and 6.27 GHz respectively. These values represent good matching of proposed antenna to a 50-ohm, thus maximum power is being transferred to antenna from feeding line.

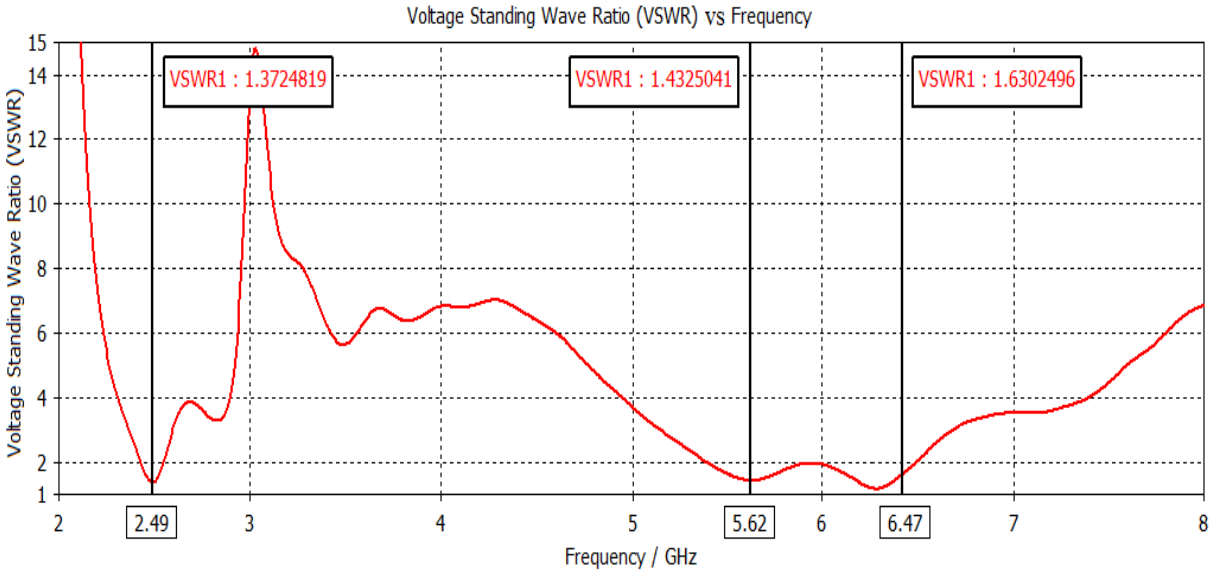

Figure 3.4 Simulated VSWR of proposed antenna.

The peak gain for the three resonant operating frequency bands viz. 2.43 – 2.54 GHz, 5.40-5.88 GHz and 6.00 - 6.47 GHz were also simulated as illustrated in Figure 3.5 The simulated peak gain has approximate values of 1.89, 4.87 and 4.14 dBi for three operating frequency bands.

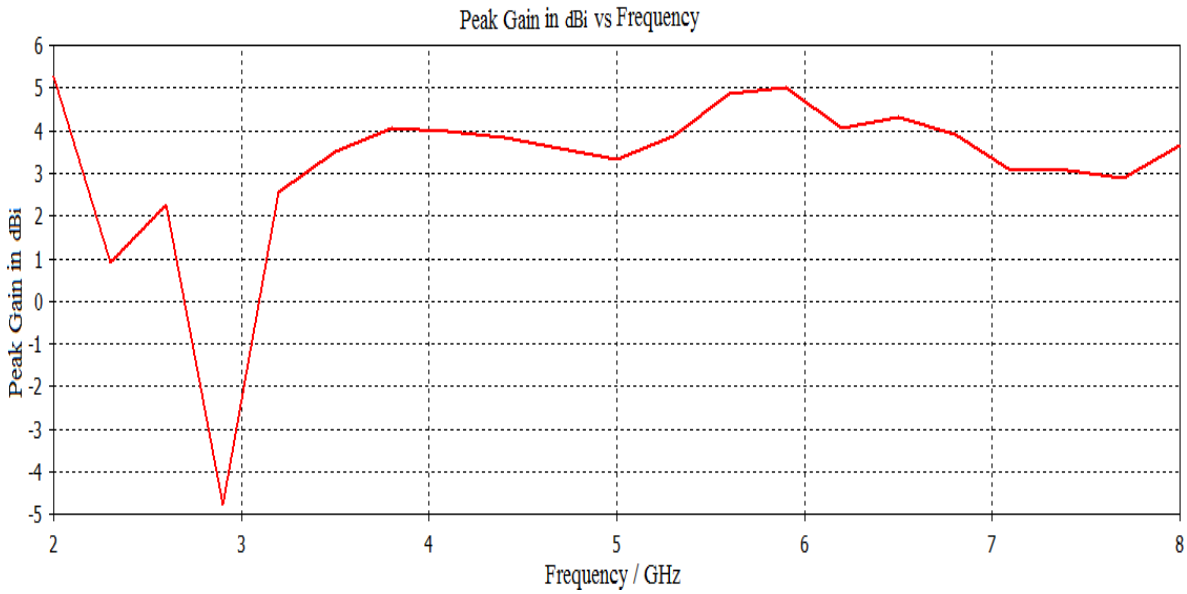

Figure 3.5 Simulated peak gain in dBi against frequency of proposed antenna.

The manual or hit and trial procedure for the optimization of antenna parameters makes the process computationally complex and inappropriate. Thus we require using an alternate strategy which makes the computation easier and gives optimized parameters that lead to effective performance of antenna prototype. One such algorithm is the DE algorithm which is used for optimizing the antenna parameters so as to get better antenna performance in terms of higher gain, larger bandwidth and better reflection coefficient discussed in next section.

3.2.2 Simulation Results for S-Parameter, VSWR and Gain with DE

Figure 3.6 illustrated the simulated reflection coefficient of proposed antenna resonating at different frequency bands using optimization algorithm. A significant improvement in the simulated results can be observed when compared with the previous simulated results without using DE algorithm that was presented in Figure 3.3, Figure 3.4, and Figure 3.5 respectively. This plot for reflection coefficient clearly indicates that proposed antenna resonates at 2.58 and 6.04 GHz. The proposed antenna with DE covers an impedance bandwidth of 354 MHz (2.40-2.75GHz), and 1179MHz (5.26–6.44 GHz) for the respective dual resonant frequencies. The optimized results show nearly a complete agreement with the resonating frequencies that have been obtained without DE. The resonating frequency of 5.62 GHz seems to have been merged with the higher frequency band (6.00 - 6.47 GHz) thus increasing the overall impedance bandwidth and reflection coefficient of proposed antenna.

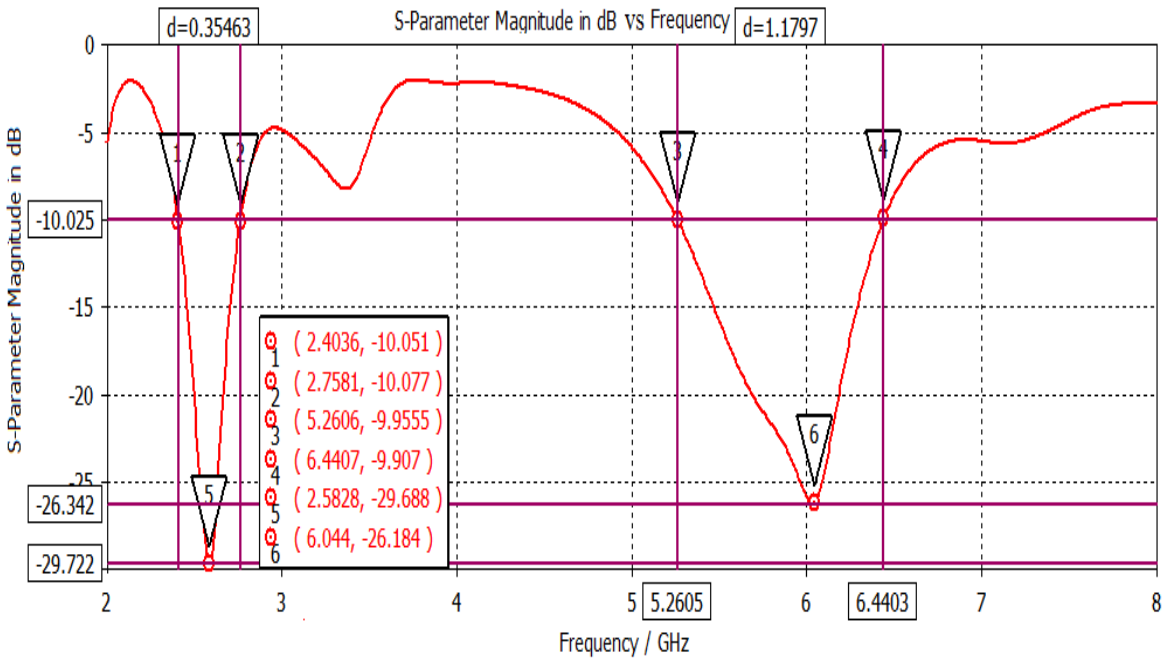

Figure 3.6 Simulated reflection coefficient of proposed antenna with DE.

Figure 3.7 shows the simulated value of VSWR for proposed antenna with DE. The VSWR was found as 1.06 and 1.10 for the two operating bands and the impedance transformation ratios were 1:1.06 and 1:1.10 for the dual band operating frequencies at 2.58 GHz and 6.04 GHz respectively. These values represent good matching of proposed antenna to a 50-ohm, thus fulfilling the condition of maximum power transfer from the feedline to antenna.

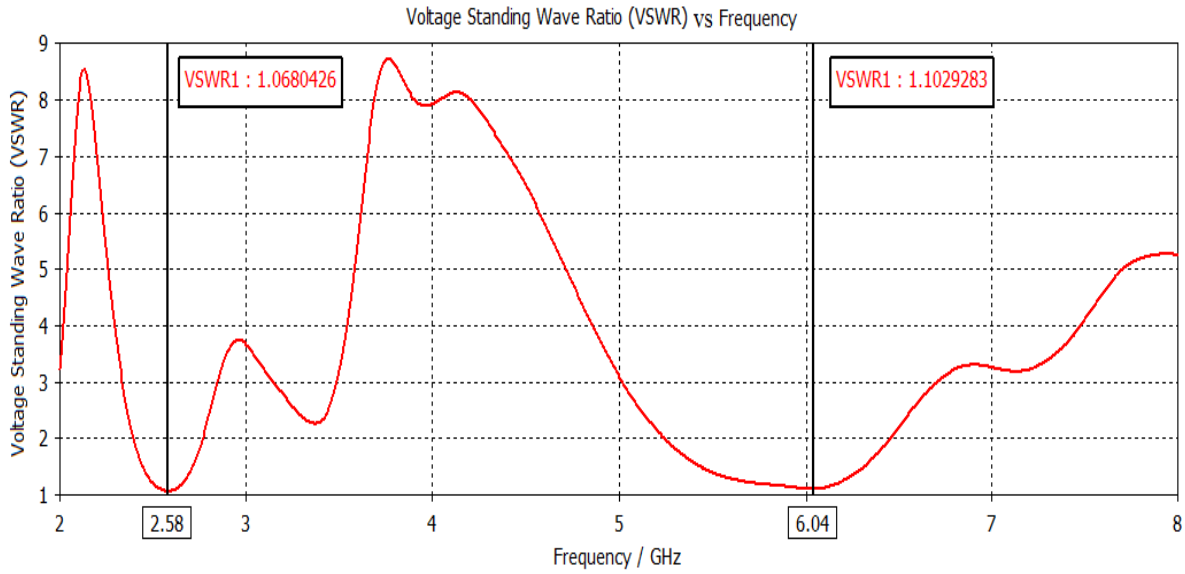

Figure 3.7 Simulated VSWR of proposed antenna with DE.

The peak gain for the two resonating frequency bands viz. 2.40 - 2.75 GHz and 5.26 – 6.44 GHz were also simulated and shown in Figure 3.8 the simulated peak gain has approximate values of 3.64 and 3.83 dBi for the two resonating frequency bands.

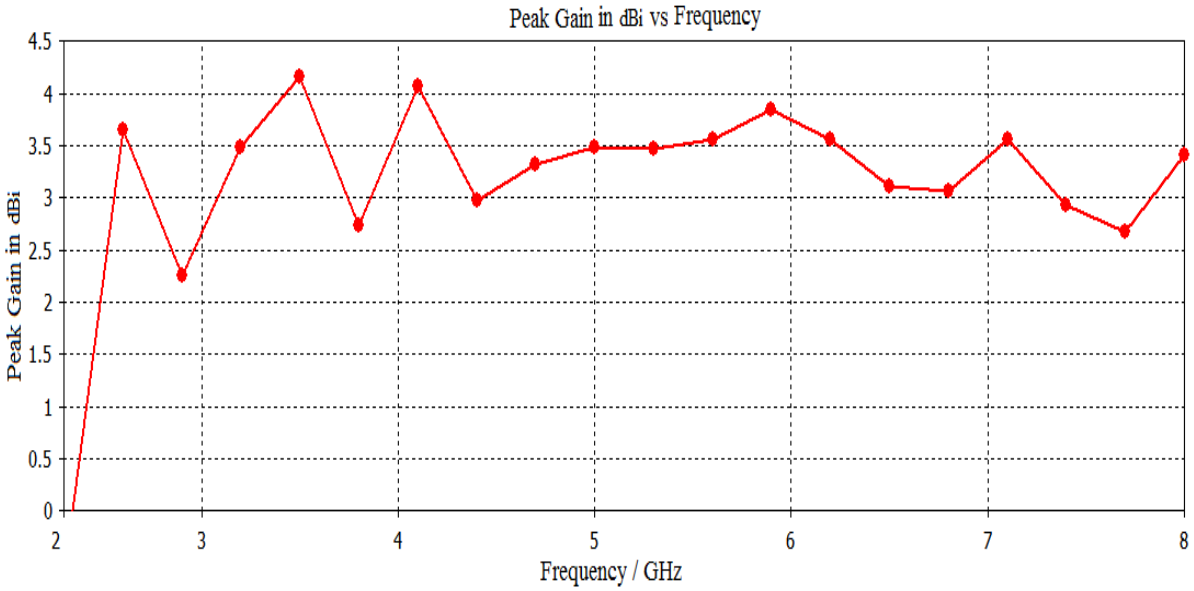

Figure 3.8 Simulated peak gain of proposed antenna with DE.

Table 3.2 represents comparison study of various antenna characteristics of proposed antenna with and without optimization. As justified from the above results, for the lower frequency band of proposed dual band antenna, -10 dB impedance bandwidth and peak antenna gain with DE is much higher than their obtained values in the antenna design without using DE. At the same time, for the upper frequency band the simulated bandwidth of antenna with DE is much larger than the bandwidth obtained without DE. Thus this simulated results prove that implementation of DE on proposed antenna has improve the antenna characteristics to great extend. This table clearly illustrates that bandwidth of proposed antenna without optimization at first operating frequency is 110 MHz where as bandwidth of proposed antenna with optimization at first operating frequency is 354 MHz. Thus significant improvement in bandwidth can be noticed. Further peak gain for first operating frequency without optimization is 1.89 dBi and with optimization is 3.64 dBi. At second operating frequency bandwidth without optimization is 470 MHz and with optimization bandwidth is obtained as 1170 MHz, a much greater bandwidth is achieved at this operating frequency with optimization. The peak gain with and without optimization is 4.14 dBi and 3.83 dBi respectively. Although gain is slightly reduced at this frequency with implementation of DE but bandwidth has shown incredible enhancement.

Bandwidth -10dB (without optimization)	Bandwidth -10dB (with optimization)	Peak Gain (without optimization)	Peak Gain (with optimization)
Frequency Range	Frequency Range	Frequency Range	Frequency Range
2.43-2.54GHz	2.40-2.75GHz	1.89dBi	3.64dBi
6.00-6.47GHz	5.26-6.44GHz	4.14dBi	3.83dBi

Table 3.2 Comparison of proposed antenna with and without optimization.

3.2.3 Current Distribution of Proposed Antenna with DE

The electromagnetic radiation pattern of the antenna can be studied through surface current distribution at the resonating frequencies 2.58 and 6.04 GHz that are displayed in Figure 3.9.

Figure 3.9 (a) and (b) illustrate the current distribution for the top and bottom plane of proposed antenna at the resonating frequency of 2.58 GHz. This plot clearly indicates that the optimized dimensions of slots S_1 and S_4 embedded in the patch are solely responsible for the bandwidth enhancement and appreciating resonance characteristics at 2.58 GHz. Figure 3.9 (c) and (d) illustrate the current distribution for the top and bottom plane of proposed antenna at the resonating frequency of 6.04 GHz. This plot shows that the position of feed line, length and width of slot in the ground plane greatly influence the resonance behavior at 6.04 GHz. However slots S_2 and S_3 incorporated in the patch also enhance the overall radiation characteristics of the proposed antenna to some extent. The radiation pattern of antenna gives the distribution of radiation characteristics for antenna in various direction of space. Figure 3.10 illustrates the radiation pattern in 3D of proposed antenna at two resonating frequencies 2.58 and 6.04 GHz. This depicts the concentration of radiation intensity on both side of antenna.

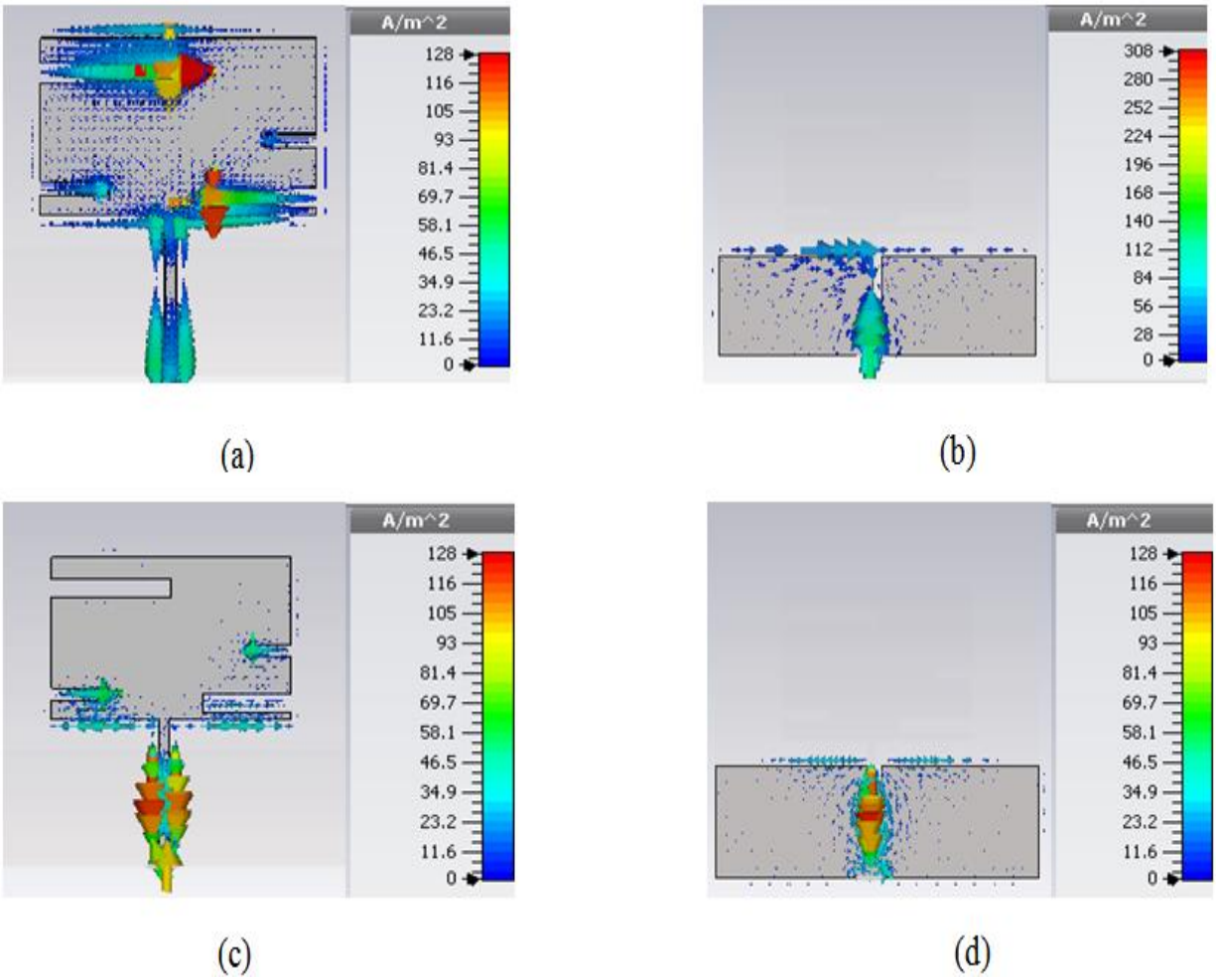

Figure 3.9 Simulated current distribution of proposed antenna with DE (a) Radiating Patch at 2.58 GHz (b) Ground plane at 2.58 GHz (c) Radiating Patch at 6.04 GHz (d) Ground plane at 6.04 GHz.

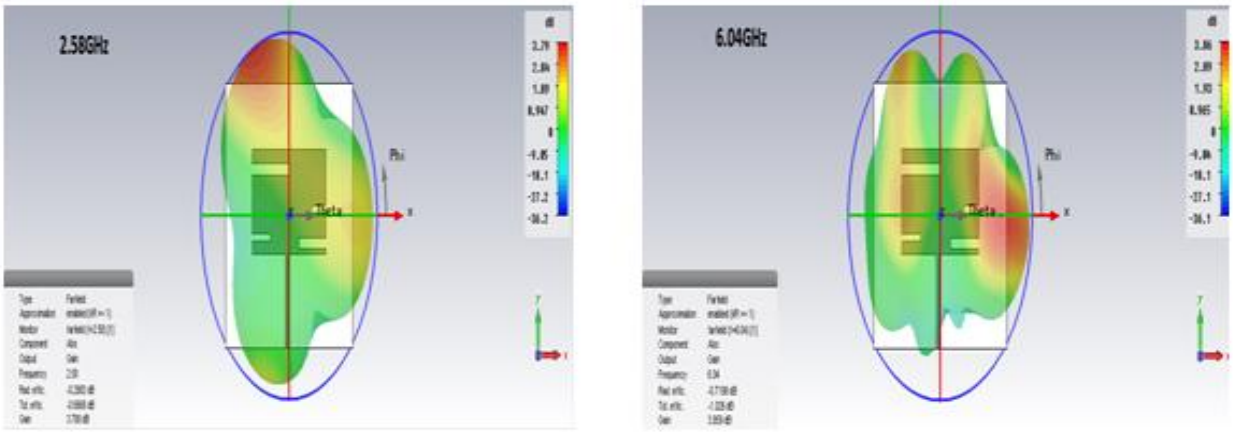

Figure 3.10 Simulated 3D radiation pattern of proposed antenna.

CHAPTER-4

DESIGN AND OPTIMIZATION OF MODIFIED T-SHAPE MICROSTRIP PATCH ANTENNA USING DIFFERENTIAL ALGORITHM FOR X AND KU BAND APPLICATIONS

In this study, a novel inset-fed slotted modified T-shape MPA with DGS is presented. This paper is a demonstration of DE, which is used to optimize the various design parameters of slotted patch antenna in accordance with diverse necessities and scenarios, and also lowers the computation complexity of antenna.

4.1 INTRODUCTION

In this work, the performance of inset-cut microstrip line fed rectangular MPA is evaluated using DE [30]. In order to see the correlation between the specific resonating frequency of antenna and its return loss, we need to define the fitness function, which can be calculated using transmission line model [31, 32]. The fitness function actually depends upon three key optimization parameters such as length, width and feed position. DE is carried out in four steps viz. Initialization, Mutation, Crossover and Selection. Mutation and Crossover are user defied parameters and have a noteworthy effect on the performance of the algorithm [33-35].

Initialization:

This search technique is a population based method, which uses NP as a population variable $X^{j}_{i,g}$, where j = 0,1,2…NP-1, i represents the size of population and g express total number of iterations that will run for each population. For initial population the lower and upper (X^{j}_{max} and X^{j}_{min}) limit of the target vector is defined. It is generated randomly from target vector if no information is available [36]. DE keeps on updating the number of population agents over each iteration.

$$X^{j}_{i,g} = X^{j}_{min} + \text{rand}(0,1) * (X^{j}_{max} - X^{j}_{min}) \qquad \text{Equation (4.1)}$$

Mutation:

A mutant vector $V_{i,g+1}$ is generated from three random vectors r1, r2 and r3. The weighted difference of any two randomly selected vectors is added to the third randomly chosen vector.

$$V_{i,g+1} = X_{r1,g} + F(X_{r2,g} - X_{r3,g}) \qquad \text{Equation (4.2)}$$

The scaling factor F is a user defined parameter and it scales the weighted difference of two randomly selected vectors and adds it to third one, ranging from 0 to 2.

Crossover:

The CR between the target vector and mutant vector is performed for generating the trial vector $U_{ji,}G+1$. CR is a user defined probability parameter ranging from 0 to 1. Trial vector inherits the parameter value from the mutant vector.

$$U_{ji,}G+1 = V_{ji,}G+1; \text{ if } (randj \leq CR)$$

$$= X_{i,}G \text{ otherwise.} \qquad \text{Equation (4.3)}$$

Selection:

Lastly, the trial vector is compared with the target vector and the best fitness value that is lower of the two becomes the target vector for the next generation. Until the termination criterion is satisfied, the same process continues.

4.2 ANTENNA DESIGN AND SIMULATION RESULTS WITH AND WITHOUT DE

Figure 4.1 shows the design specifications of different configurations of proposed antenna. The proposed antenna is mounted on a low-loss thin sheet of insulating dielectric substrate named Epoxy Glass-FR4, with thickness 1.56 mm, permittivity ϵ_r=4.4 and loss tangent tan δ = 0.025. All these specifications for substrate are considered as the part of material parameters window on CST MWS V14.0. On one side, this dielectric is covered with metal generally known as ground and on the other side of the substrate moderately metalized covering is present, which is known as patch and all the antenna patterns are being printed on the patch. The feed line and patch are fabricated on the upper side of the substrate. In this proposed antenna design, inset-cut feed arrangement is used, which is at the depth of approximately half of the length of ground plane, that feeds the radiator. The antenna configurations are: L_g=L_s=20 mm, W_g=W_s=11 mm, L_p=10.75 mm, W_p=8 mm, L_{sp}=2 mm, W_{sp}=0.75 mm and L_f =10 mm. The patch and ground has slots etched on them.

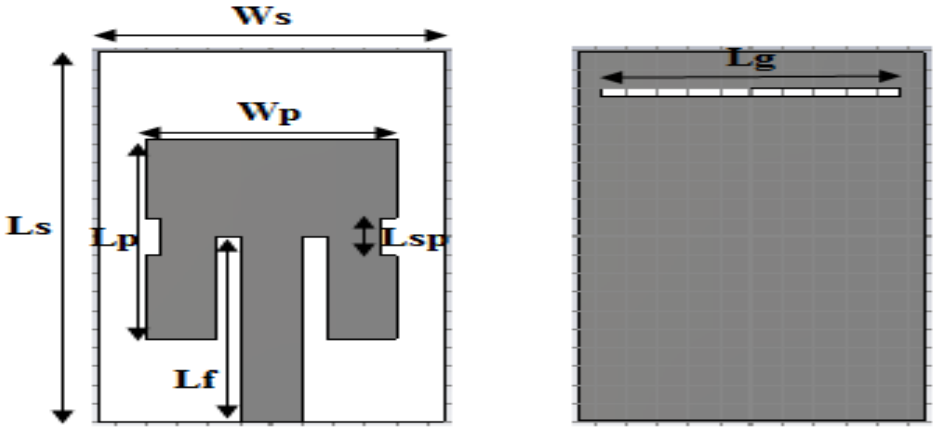

Figure 4.1 Design configurations of the proposed antenna with front view and back view.

4.2.1 Simulation Results for S-Parameter, VSWR and Gain without DE

The reflection coefficient as well as VSWR can be used to evaluate the matching characteristics of an antenna. Reflection coefficient should be effectively less than -10 dB which is approximately equal to VSWR 2:1, as this value of reflection coefficient is considered to be the most suitable for good antenna performance. Further, smaller is the value of VSWR of an antenna, more power is accepted by the antenna and less power is reflected back. Hence antenna performance becomes better Figure 4.2 illustrates the dual band frequency behavior of the proposed antenna design for |S11|< -10 dB, viz. Band 1 ranging from 11.53 to 12.12 GHz with resonating frequency at 11.82 GHz and Band II ranging from 15.45 to 16.54 GHz with resonating frequency at 16.04 GHz. The bandwidth covered by the first and second frequency band is approximately 590 MHz and 1080 MHz respectively.

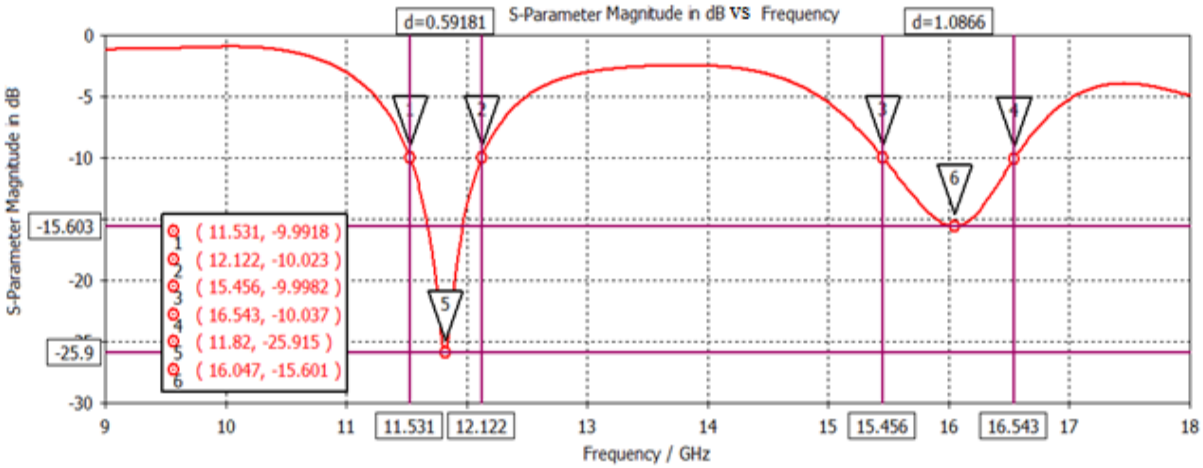

Figure 4.2 Reflection coefficient of proposed antenna without DE.

Figure 4.3 shows that the variation of VSWR is < 2 over the two frequency bands. The value of VSWR at first resonant frequency 11.82 GHz is 1.10 and at second resonant frequency 16.04 GHz is 1.39.

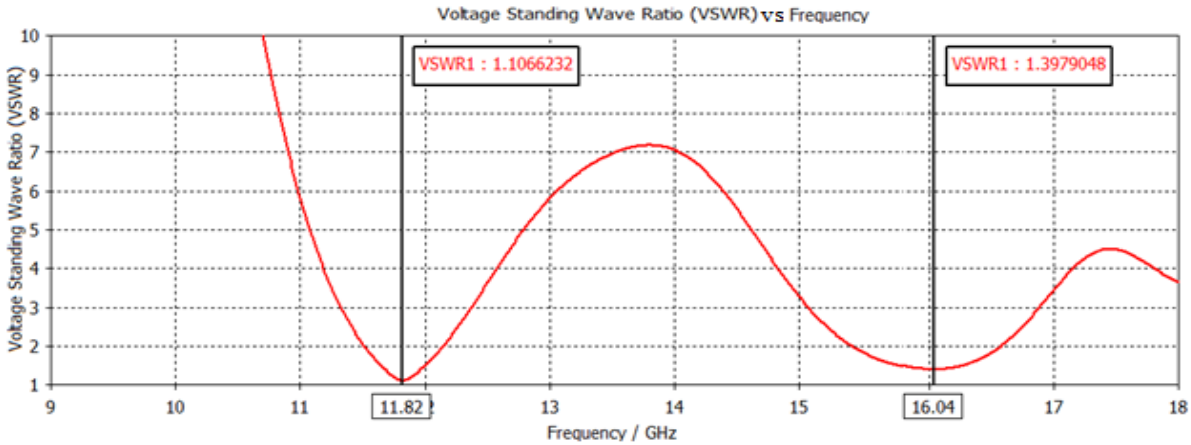

Figure 4.3 VSWR of proposed antenna without DE.

Figure 4.4 shows the simulated peak gain Vs frequency curve for the proposed antenna. The peak gain is 3.10 dBi in the first frequency band (11.53-12.12 GHz) and 1.55 dBi in the second frequency band (15.45-16.54GHz).

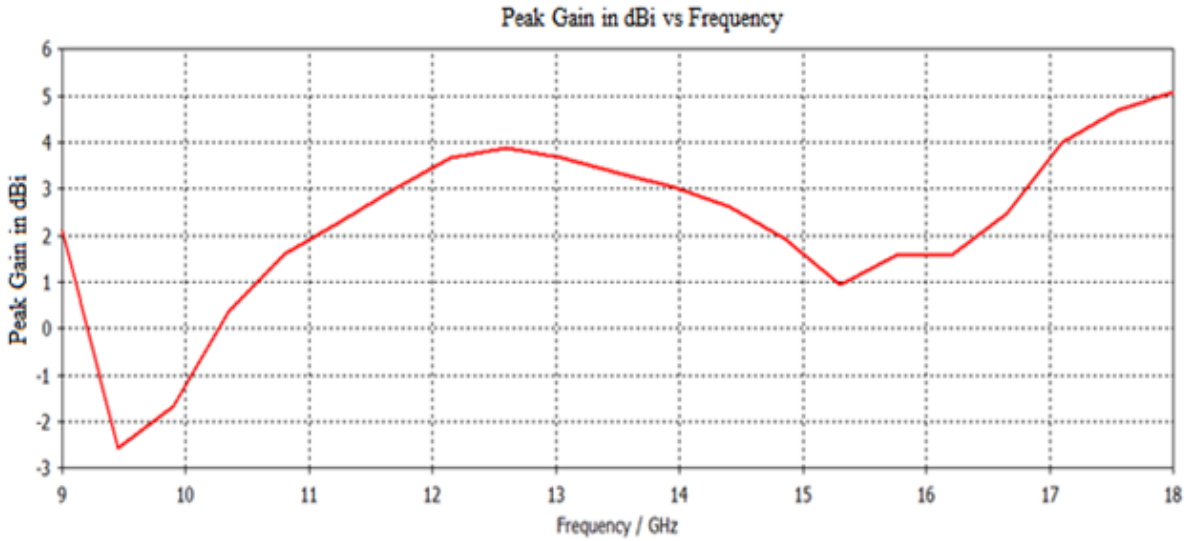

Figure 4.4 Peak gain in dBi of proposed antenna without DE.

To improve antenna performance characteristics such as reflection coefficient, bandwidth and gain, an optimization algorithm is required that optimizes the antenna parameters such as length and width of patch, ground and slots. To overcome these shortcomings of manual optimization, algorithmic optimization is more preferable as it reduces the complexity of calculations and gives better results in less time. The optimization algorithm that we will use in this work DE is discussed in next section.

4.2.2 Simulation Results for S-Parameter, VSWR and Gain with DE

Figure 4.5 shows the simulated reflection coefficient of the proposed antenna with DE. This plot clearly indicates a significant improvement in reflection coefficient with the difference of approximately 2.3 dB and 4.2 dB for the lower and upper band respectively as compared to the non-optimized proposed antenna. At the same time, impedance bandwidth has been increased by 5% and 0.66% for the lower and upper band respectively in comparison to the non-optimized antenna. The first frequency band ranges from 10.90 to 12.04 GHz with resonating frequency at 11.76 GHz and second frequency band ranges from 15.06 to 16.23 GHz with resonating frequency at 15.67 GHz. The bandwidth covered by first frequency band is 1140 MHz and second frequency band covers the bandwidth of 1170 MHz. Figure 4.6 shows the variation in the value of VSWR for the resonant frequency 11.76 GHz and 15.67 GHz.

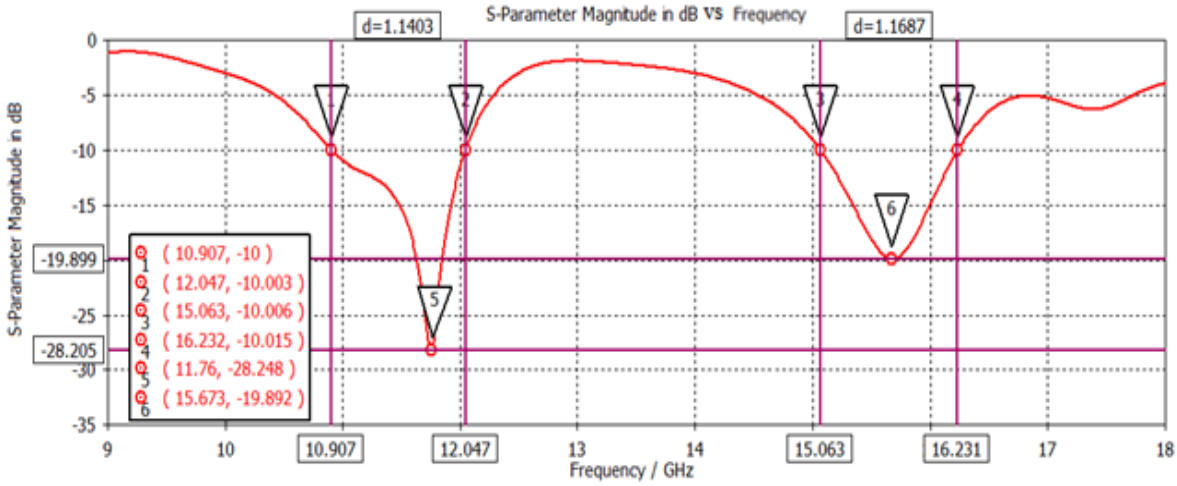

Figure 4.5 Reflection coefficient at dual-frequency bands of proposed antenna with DE.

Figure 4.7 shows the simulated peak gain of 5 dBi and 1.59 dBi for the two resonating frequencies 11.76 GHz and 15.673 GHz respectively which is relatively good. Thus optimized simulated results of the proposed antenna with DE show the stabilized improvement in the reflection coefficient, bandwidth and gain.

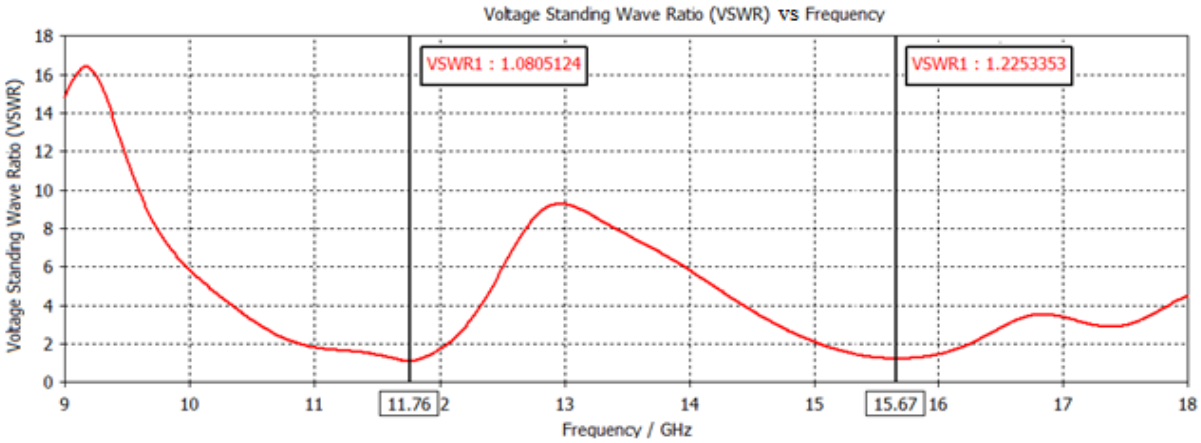

Figure 4.6 VSWR of proposed antenna with DE.

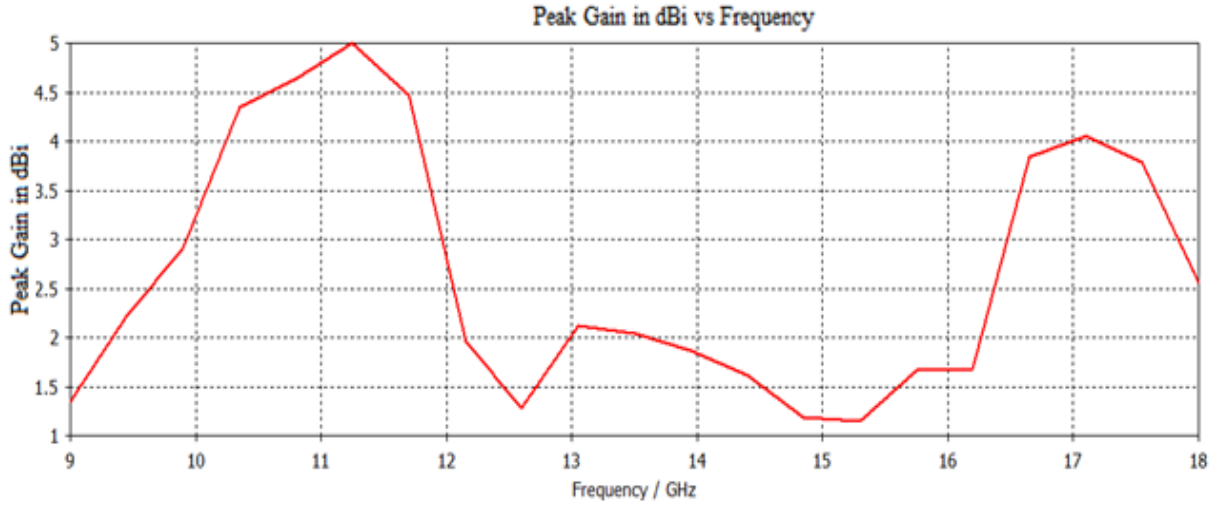

Figure 4.7 Peak gain in dBi of proposed antenna with DE.

4.2.3 Current Distribution of Proposed Antenna with DE

Figure 4.8 (a-b) shows the distribution of current on the excited resonant modes of the proposed antenna at two resonant frequencies 11.76 GHz and 15.67 GHz. Figure 4.8 (a) shows the surface current distribution on patch and ground of proposed antenna at the resonating frequency 11.76 GHz. This figure clearly shows that the horizontal slot in the ground plane is responsible for the antenna to resonate at 11.76 GHz. Figure 4.8 (b) shows the surface current distribution on patch and ground of proposed antenna at the resonating frequency 15.67 GHz. This figure represents that inset-cut feed line exciting the patch is responsible for the resonating frequency at 15.67 GHz. However the slots embedded in the patch are also responsible for the overall improvement in the radiation characteristics of antenna. The radiation pattern of the antenna describes the variation of the radiation intensity at large distances everywhere in distinctive directions of space. To demonstrate the radiation from our transceiver, we outline in

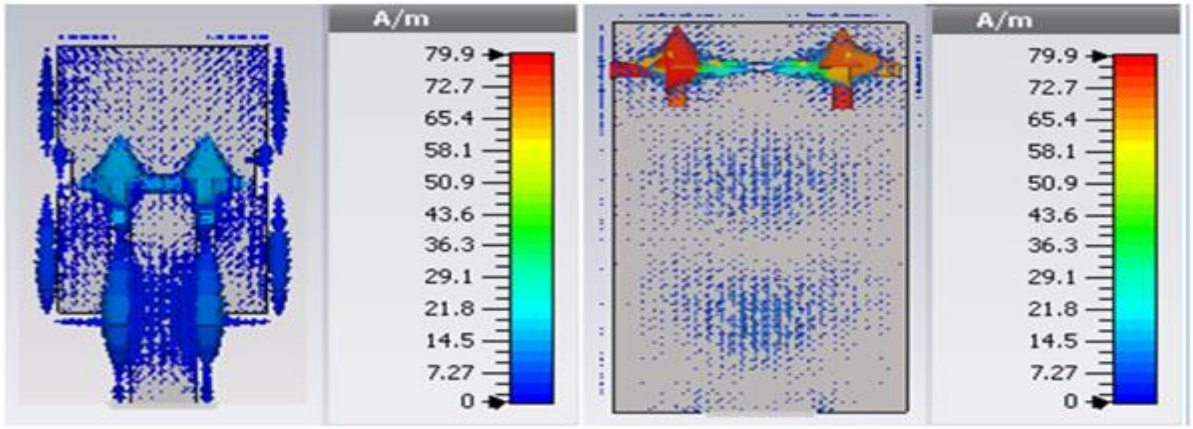

(a)

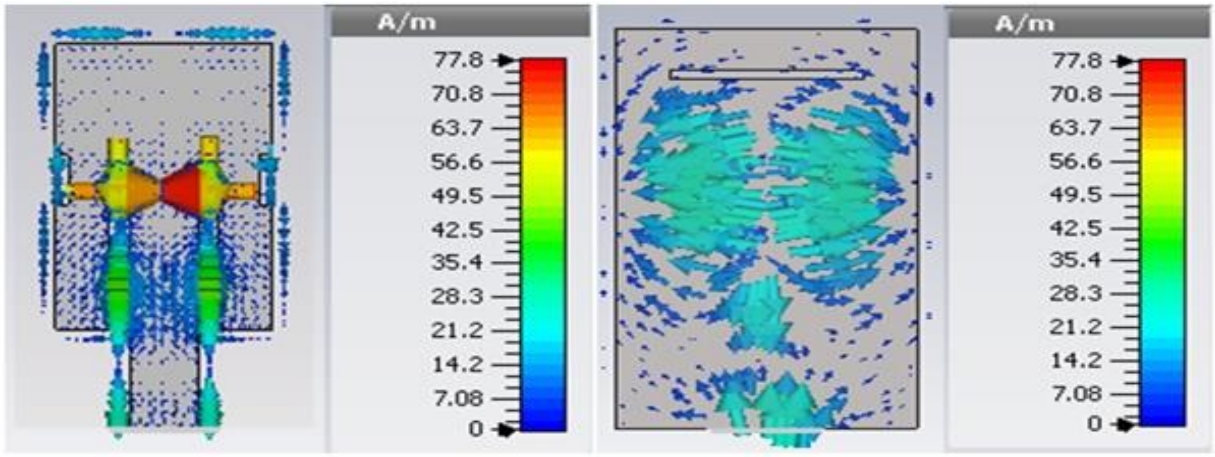

(b)

Figure 4.8 Simulated surface current distribution of proposed antenna at (a) 11.76 GHz (b) 15.67 GHz.

Figure 4.9 (a-b) the 3D radiation design of the proposed antenna at resonant frequencies 11.76 and 15.67 GHz. Table 4.2 speaks to the comparison investigation of proposed antenna with and without optimization. This table clearly portrays the detectable change in the bandwidth and peak gain that is acquired after the usage of DE algorithm.

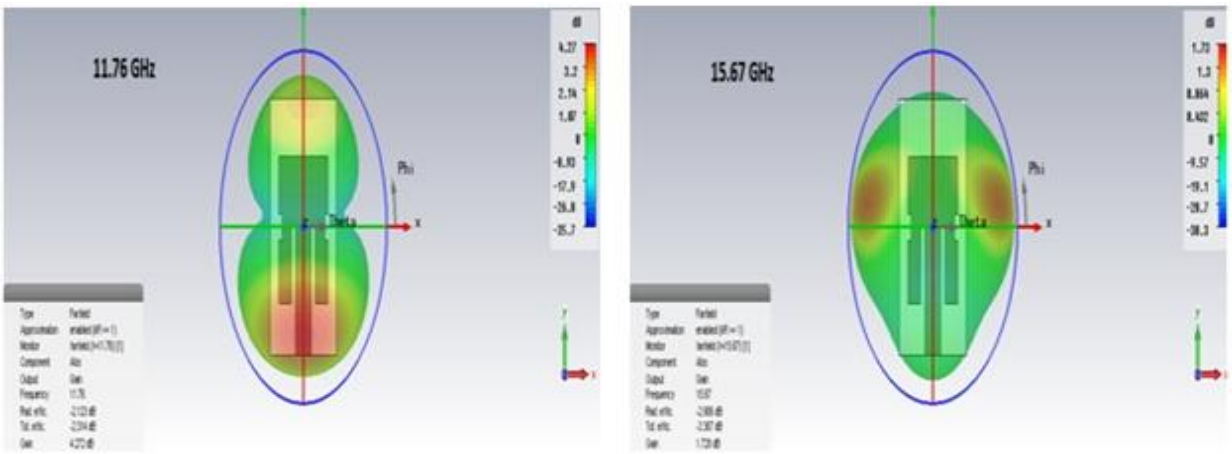

(a) (b)

Figure 4.9 Simulated 3D Radiation pattern of proposed antenna with DE at (a) 11.76GHz (b) 15.6 GHz.

Bandwidth -10dB (without optimization)	Bandwidth -10dB (with optimization)	Peak Gain (without optimization)	Peak Gain (with optimization)
Frequency Range	Frequency Range	Frequency Range	Frequency Range
11.53- 12.12GHz	10.90-12.04GHz	3.10dBi	5dBi
15.45-16.54GHz	15.06-16.23GHz	1.55dBi	1.59dBi

Table 4.1 Comparison of proposed antenna with and without optimization.

CHAPTER-5

DESIGN OF HAND-FAN SHAPED MICROSTRIP PATCH ANTENNA WITH U-SLOT DGS FOR L-BAND AND S-BAND APPLICATIONS

In this article a novel MPA design for ultra-wide band (UWB) applications is presented. The proposed hand-fan shaped MPA with double U-slot DGS fabricated on a FR4 substrate which is wide enough to cover the required ultra wide band frequency range. The proposed antenna covers the L-band and S- band applications.

5.1 INTRODUCTION

The communication process is dependent on antenna performance for it is the fundamental device for sending and receiving the information. Thus effective and reliable antennas are required for the process of communication. The demands for compact size with less weight and low cost antennas are continuously increasing due to which there is a rapid progress in wireless broadband technologies [37]. Such antennas include patch antennas, slot antennas and folded dipole antenna [38]. Each antenna requires an appropriate design to transmit the signal effectively and it also possesses specific advantages and disadvantages. Microstrip antenna is one such antenna which has low profile, light weight, high performance and easy fabrication characteristics. These smart features of microstrip antenna increase its popularity that prompted various researchers to perform great and vast research on it [39, 40].

5.2 ANTENNA DESIGN AND SIMULATION RESULTS

Figure 5.1 (a-b) shows the front view and back view of proposed MPA respectively. It is a basic rectangular patch antenna which has gone through number of changes to achieve the desired results. This antenna is simulated using FR4 substrate with dielectric constant $\epsilon r = 4.4$ and loss tangent = 0.0025. The patch is considered to be a radiating element. The microstrip feedline which is the least difficult of all the feeding strategies is utilized as a feeding component for this antenna configuration keeping in mind the end goal to accomplish a decent impedance of 50 ohms.

The over size of the antenna is 98 x 74 mm^2 and substrate used have a thickness of 1.57 mm. The radiating material is designed in such a way that it resembles the hand-fan shape structure. Slots s1, s2 and s3 are being expelled from the patch to show signs of improvement in antenna characteristics. The utilization of partial ground and stub in the feedline permits

the broadening of the bandwidth and acquiring better impedance matching. Table 5.1 gives the geometrical configuration of all parameters that are used for designing proposed antenna.

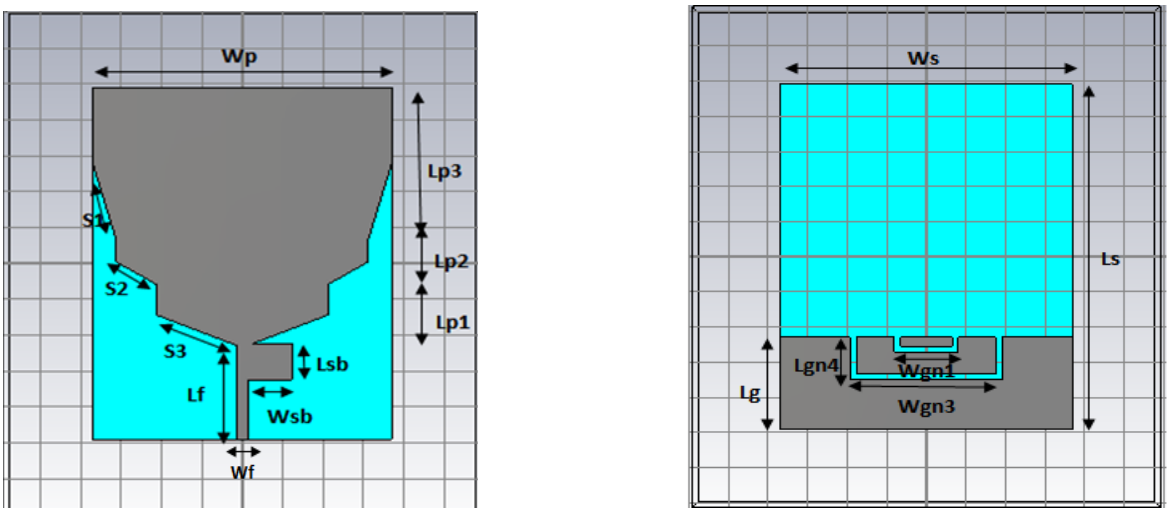

(a) (b)

Figure 5.1 Geometrical configuration of proposed (a) Front View – Radiating structure (b) Back View – partial DGS plane.

Elements	Dimensions (mm)
Ground plane	$W_g = 74$; $L_g = 26.2$ $W_{gn1} = 16.3$; $L_{gn1} = 1.6$ $W_{gn2} = 38.4$; $L_{gn2} = 4.3$ $W_{gn3} = 74$; $L_{gn3} = 1.6$
Patch	$W_p = 74$; $L_{p1} = 17.1$ $L_{p2} = 1$; $L_{p3} = 42.3$
Feedline	$W_f = 2.8$; $L_f = 26.7$

Table 5.1 Geometrical Configuration of proposed antenna.

5.2.1 Simulation Results of S-Parameters, VSWR and Gain

Figure 5.2 shows the plot of S-parameter against frequency for the proposed antenna. The best outcomes are accomplished at –10 dB for better antenna execution and the reflection coefficient is considered to be the best at this coefficient esteem. We can presume that the slots is the DGS plane and in the radiating patch is passable for more prominent development in frequency band and in value of S11 which brings about ultra wide band structure.

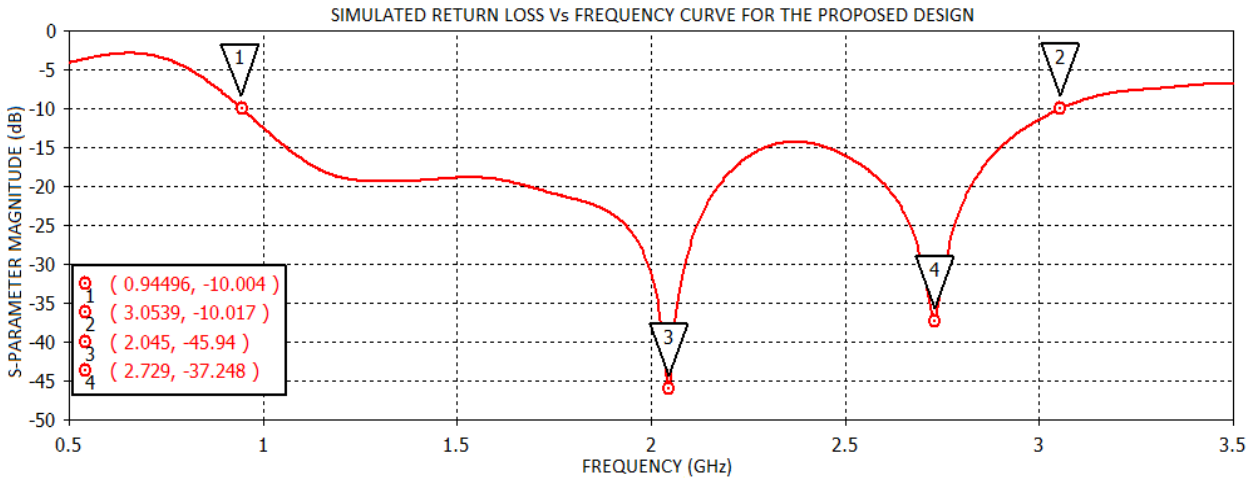

Figure 5.2 Simulated S-parameter curve of proposed antenna

The simulated result of the proposed antenna shows the ultra wide band frequency range of 0.94 - 3.05 GHz with their resonating frequency at 2.04 GHz and 2.72 GHz with impedance bandwidth of 2110 MHz.

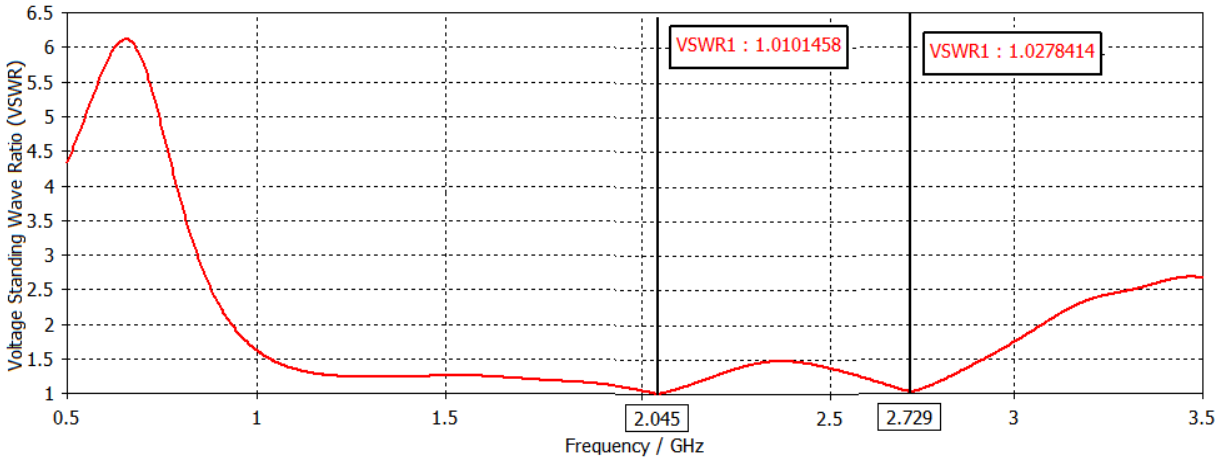

Figure 5.3 Simulated VSWR of proposed antenna.

Figure 5.3 shows the value of VSWR for proposed antenna at dual band frequency. VSWR depicts the power reflected from the antenna; it is a function of reflection coefficient. Smaller the estimation of VSWR more is the power conveyed to the antenna as it will have better matching with the transmission line. The estimation of VSWR ought to be less than 2, ideal estimation of VSWR is 1 which is a perfect esteem and for this situation no power is reflected from the antenna. For this proposed antenna VSWR at dual resonant frequencies is illustrated in Figure 5.4 at first resonant frequency 2.04 GHz the value of VSWR is 1.01 and at the second resonant frequency 2.72 GHz the value of VSWR is 1.02 , further the impedance transformation ratio for two respective resonant frequencies are 1:1.01 and 1:1.02. This represents power is effectively delivered to the antenna and very less power is reflected for better performance of antenna.

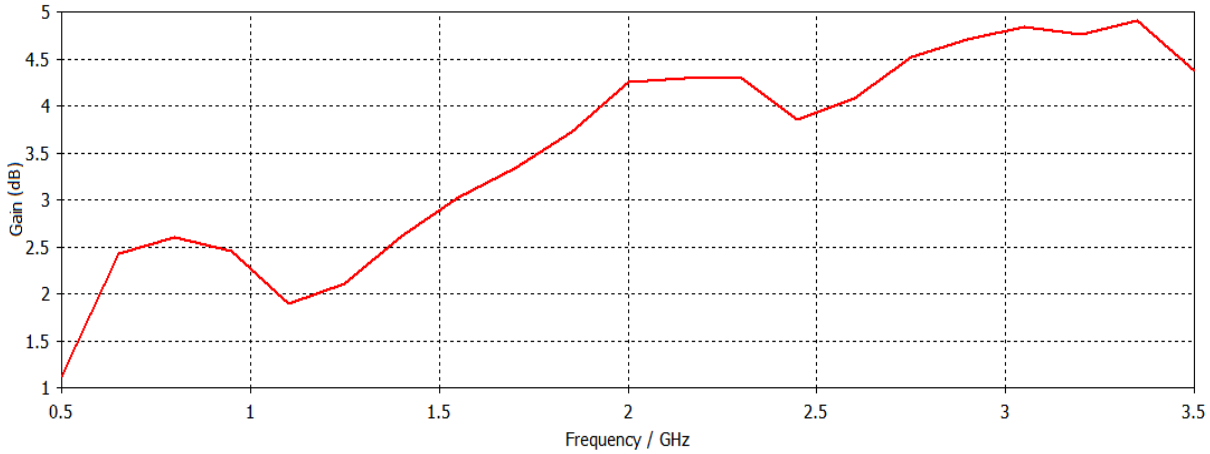

Figure 5.4 Simulated peak gain of proposed antenna

The technical insertion of the slots in the radiating element or partial DGS plane affects the overall performance of the antenna. Figure 5.4 demonstrates the peak gain of proposed antenna covering the ultra wide band frequency range from 0.94 - 3.05 GHz. Gain is the key number in the execution of the antenna which is identified with its directivity and efficiency of the antenna. The peak gain of proposed antenna in obtained frequency range is 4.83dB. This is considered to be a good gain for better antenna performance.

5.2.2 Current Distribution of Proposed Antenna

Figure 5.5 (a-b) illustrates the surface current distribution of proposed antenna on patch and plane for the two resonating frequencies. It depicts the excitation on the resonant mode of proposed antenna. The detail of the surface current on the two resonating frequencies of proposed antenna is demonstrated as follows: Figure 5.5 (a) illustrates the surface current distribution on patch and DGS plane of proposed antenna at resonant frequency 2.04 GHz. This figure illustrates the feedline with stub protruded from it for exciting patch is responsible for first resonant frequency. The slots in the partial DGS plane also affect the overall performance of proposed antenna.

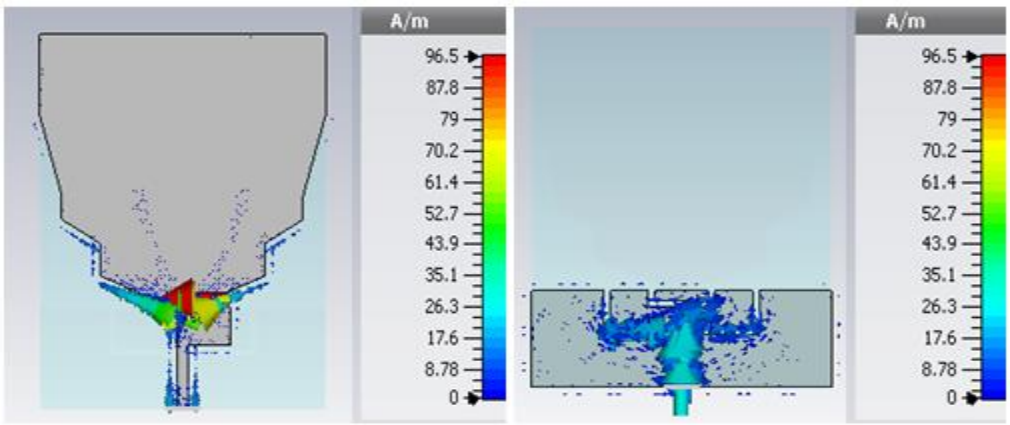

(a)

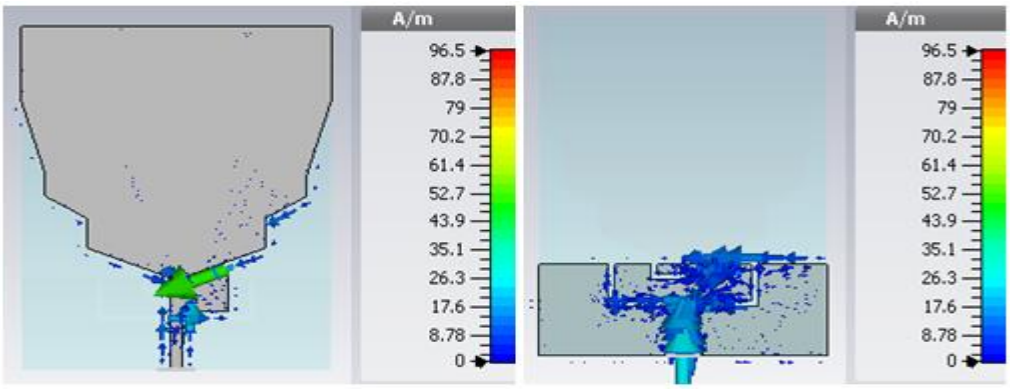

(b)

Figure 5.5 Surface current distribution (a) On patch and DGS plane of proposed antenna at resonant frequency 2.04 GHz (b) On the patch and ground plane of proposed antenna at resonant frequency 2.72 GHz.

Similarly, Figure 5.5 (b) illustrates the surface current distribution on patch and ground plane of proposed antenna at resonant frequency 2.72 GHz. This figure shows the lower edge of patch and feedline are responsible for second resonant frequency. The slots in the partial DGS plane also affect the overall performance of proposed antenna. Thus from the current distribution it can be concluded that all the parameters of antenna including slots embedded in the patch and ground responsible for improving the radiation characteristics of antenna. Figure 5.6 (a-b) shows the 3D radiation pattern of proposed antenna at resonant frequency 2.04 GHz and 2.72 GHz. The radiation pattern describes the variation in the radiation intensity of antenna in various heading of space

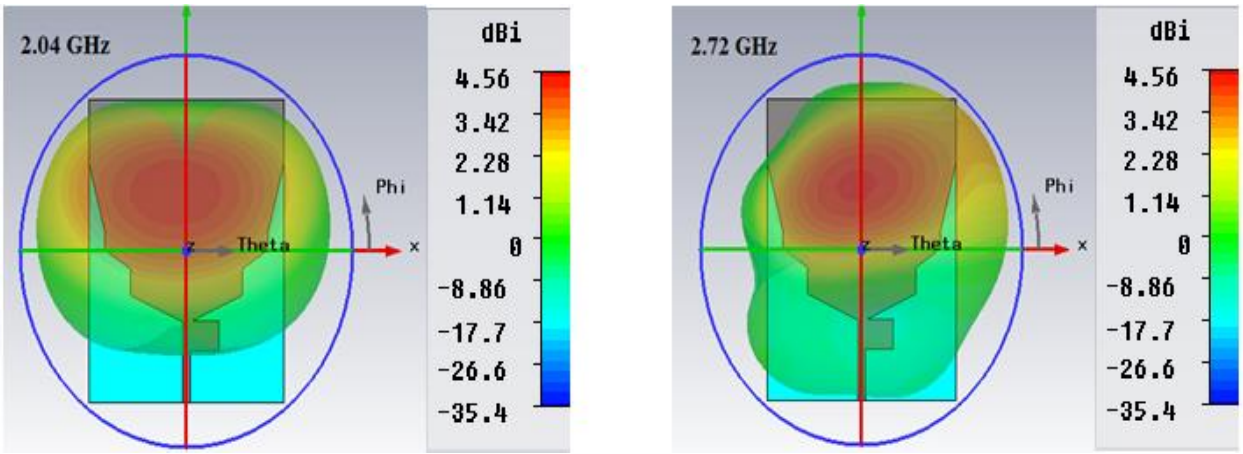

(a) (b)

Figure 5.6 3D Radiation pattern of proposed antenna at (a) 2.04 GHz (b) 2.72 GHz.

CHAPTER 6

FABRICATION AND TESTING OF PROPOSED ANTENNAS

This chapter deals with fabrication and testing of the proposed antennas that were simulated in Chapter 3, 4 and 5. This is carried out in order to check the applicability of proposed antennas. Firstly the fabrication process is clarified and afterward simulated and measured outcomes are looked at. The dielectric substrate material utilized was an Epoxy Glass-FR4 and a wet-etching procedure based conventional photolithography technique is being acknowledged for fabrication of antenna. The reflection coefficient and radiation intensity of antenna is measured using Aglient E5071C vector network analyzer (VNA) and Anechoic Chamber respectively.

6.1 FABRICATION PROCEDURE

This section describes the flowchart for the fabrication procedure of proposed antennas in sequential manner.

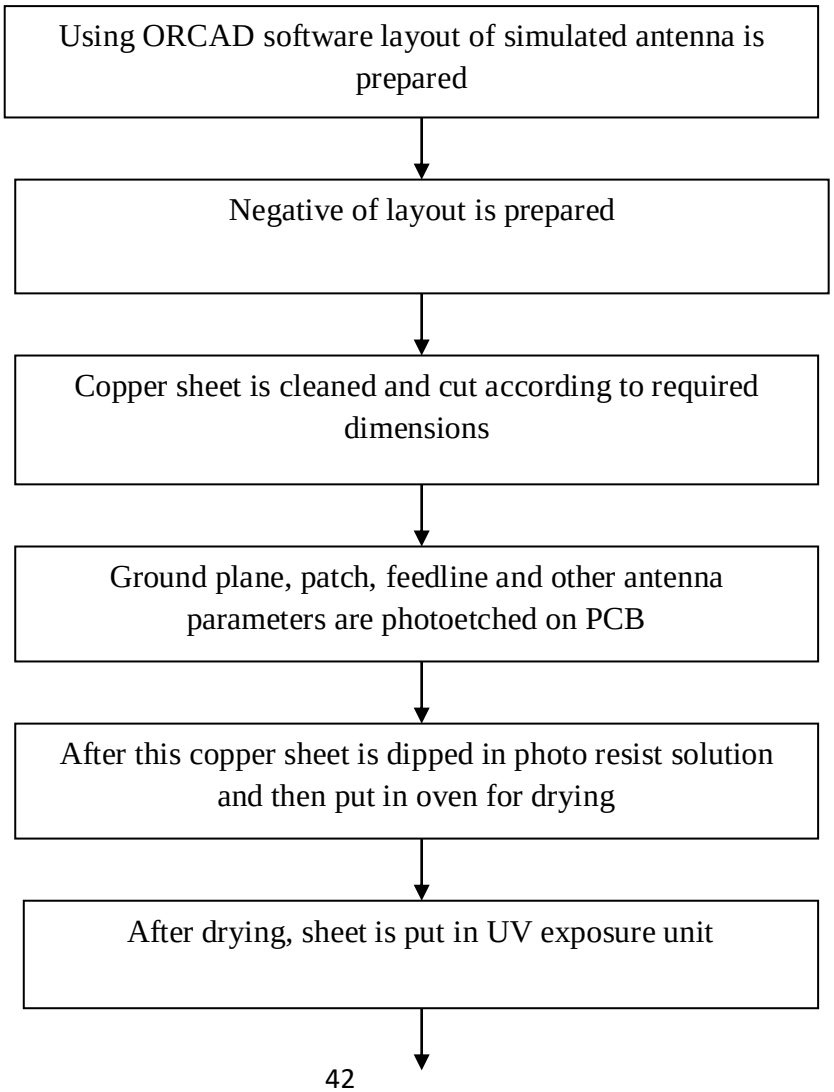

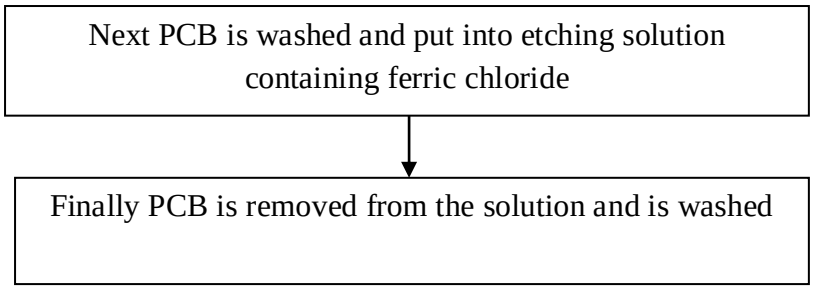

Figure 6.1 Flowchart for fabrication procedure of antenna.

6.2 TESTING OF FABRICATED ANTENNA

The reflection coefficient is tested using Aglient E5071C VNA, with the frequency ranging from 0 - 20GHz. Figure 6.2 shows the photograph of the Aglient vector network analyzer.

Figure 6.2 Photograph of Aglient E5071C VNA.

6.3 FABRICATION OF DUAL-BAND RECTANGULAR MICROSTRIP PATCH ANTENNA

Figure 6.3 shows the photograph of fabricated dual-band rectangular MPA. The fabrication of the prototype antenna was done with the help of available photolithography method with wet-etching facility as mentioned above in flowchart.

(a)

(b)

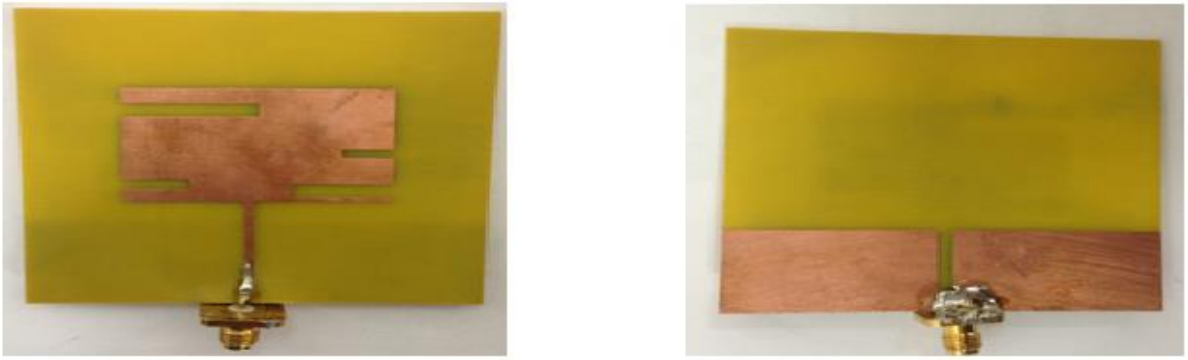

Figure 6.3 The Photograph of fabricated proposed antenna (a) Top view with connector (b) Bottom view without connector (c) Top view with four-hole SMA connector (d) Bottom View with four-hole SMA connector.

6.3.1 Comparison of Simulated and Measured S-parameter Radiation Pattern and Gain of Proposed Antenna

Figure 6.4 illustrates the comparison result of the simulated and measured reflection coefficient for proposed antenna. The measured results of reflection coefficient for proposed antenna at two resonant frequencies were 2.53 and 5.77 with their respective value of reflection coefficient obtained as -24.75 dB and -27.82 dB. The measured results of two operating frequency bands for impedance bandwidth were around 340 MHz (2.34–2.68 GHz) and 1040 MHz (5.28–6.32 GHz). The simulated and measured results show a good agreement of proposed antenna. The resonating frequency is observed to be shifted; fabrication errors, interference and noise, further connector and antenna feeder's mismatching could be the cause for shifting in experimental results.

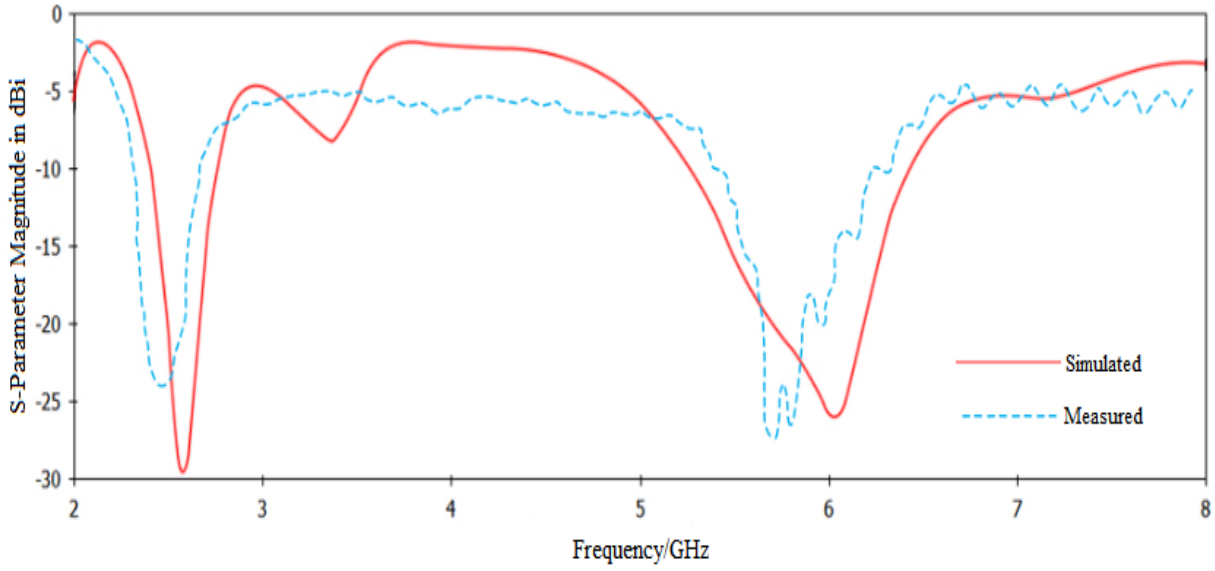

Figure 6.4 The comparison result of the simulated and measured reflection coefficient for proposed antenna

Figure 6.5 the simulated and measured E-plane and H-plane in 2D radiation pattern for proposed antenna resonating at 2.53 and 5.77 GHz. The focus of radiation for proposed antenna is on both the sides. Figure 6.6 represents the peak gain for simulated and measured results of proposed antenna and clearly indicates the closeness of the values of gains at the different frequencies over the entire frequency band.

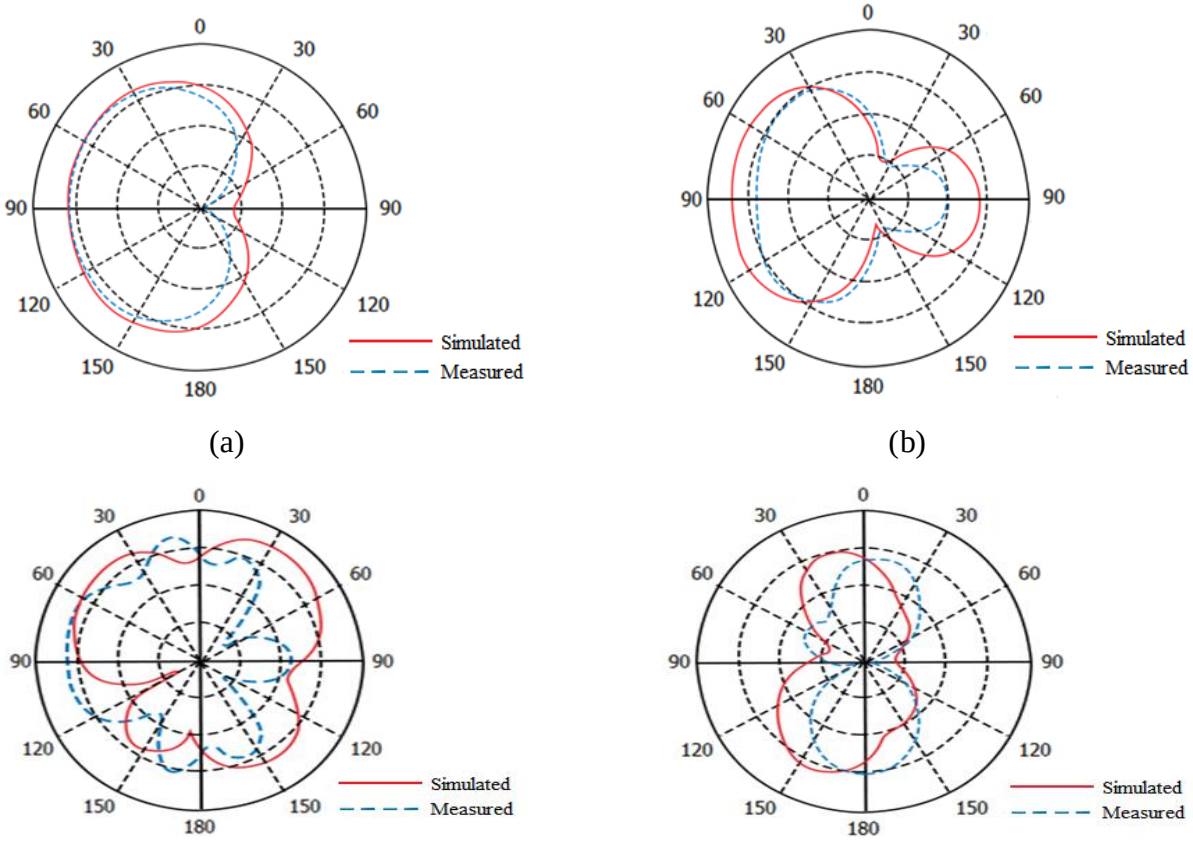

Figure 6.5 Comparison of Simulated and measured radiation pattern (a-b) 2.53 GHz (c-d) 5.77.

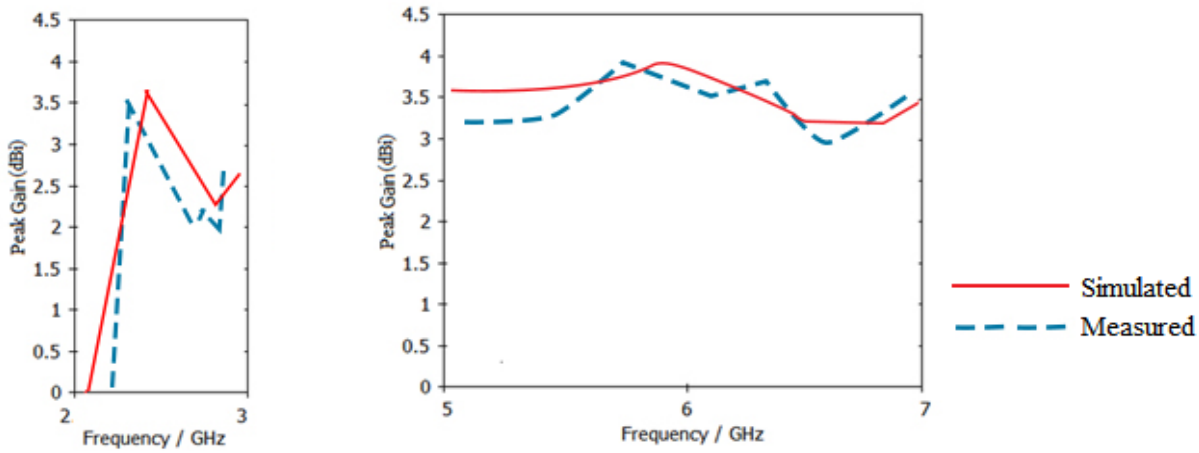

Figure 6.6 Comparison between simulated and measured peak gain of proposed antenna.

6.4 FABRICATION OF MODIFIED T-SHAPE MICROSTRIP PATCH ANTENNA

Figure 6.7 shows the photograph of fabricated modified t-shape MPA using the technique mentioned above in the flowchart for fabrication procedure.

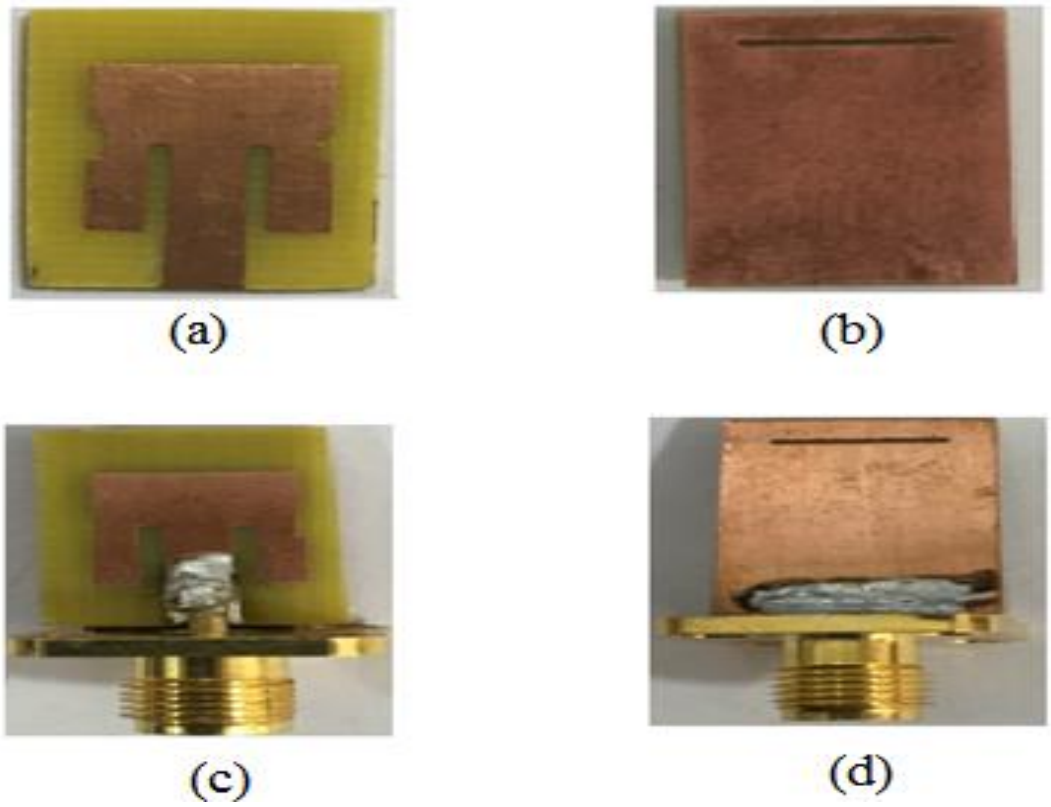

Figure 6.7 The photograph of proposed antenna (a) front view (b) back view (c) front view with connector (d) back view with connector.

6.4.1 Comparison of Simulated and Measured S-parameter and Radiation Pattern of Proposed Antenna

Figure 6.8 illustrates the comparison between simulated and measured after effects of the proposed antenna. The measured outcomes show that the proposed antenna covers the frequency range of 11.13-11.82 GHz and 15.77-16.89 GHz with their respective bandwidths of 690 MHz and 1120 MHz with their respective operating frequencies at 11.47 GHz and 16.27 GHz. The shift in resonating frequencies is because of the manufacturing mistakes, obstructions, noise and incompatibility between the connector and the antenna feeder. However a decent understanding between the measured and simulated results is acquired. Figure 6.9 demonstrate the comparison between simulated and measured 2D radiation pattern of the proposed antenna for E-plane and H-plane at 11.47 and 16.27 GHz respectively. For vertical and horizontal polarization, E-plane and H-plane should be 90 degree apart. A close agreement between the simulated and measured results has been visualized for both the resonating frequencies.

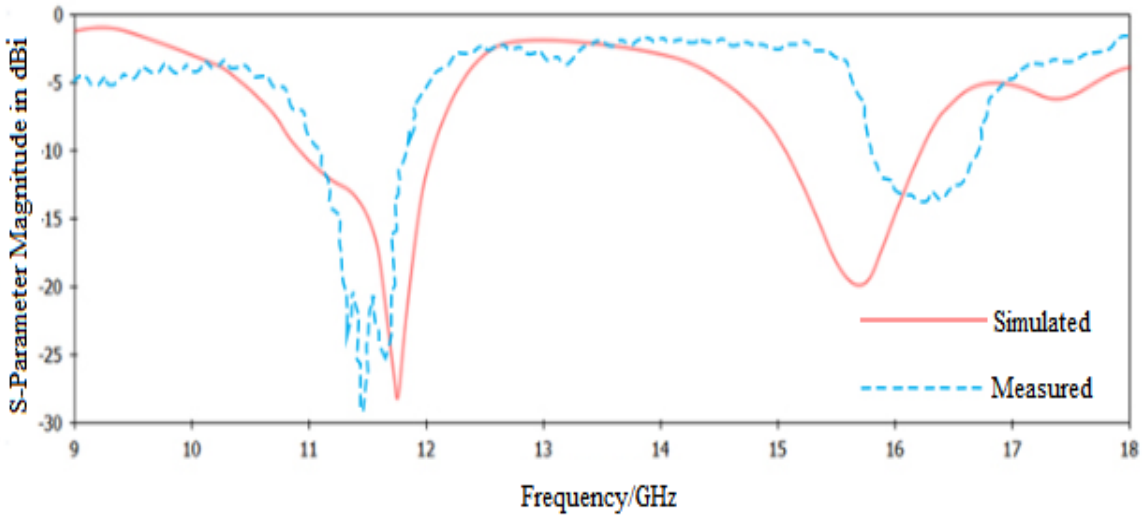

Figure 6.8 The Comparison of simulated and measured reflection coefficient for proposed antenna.

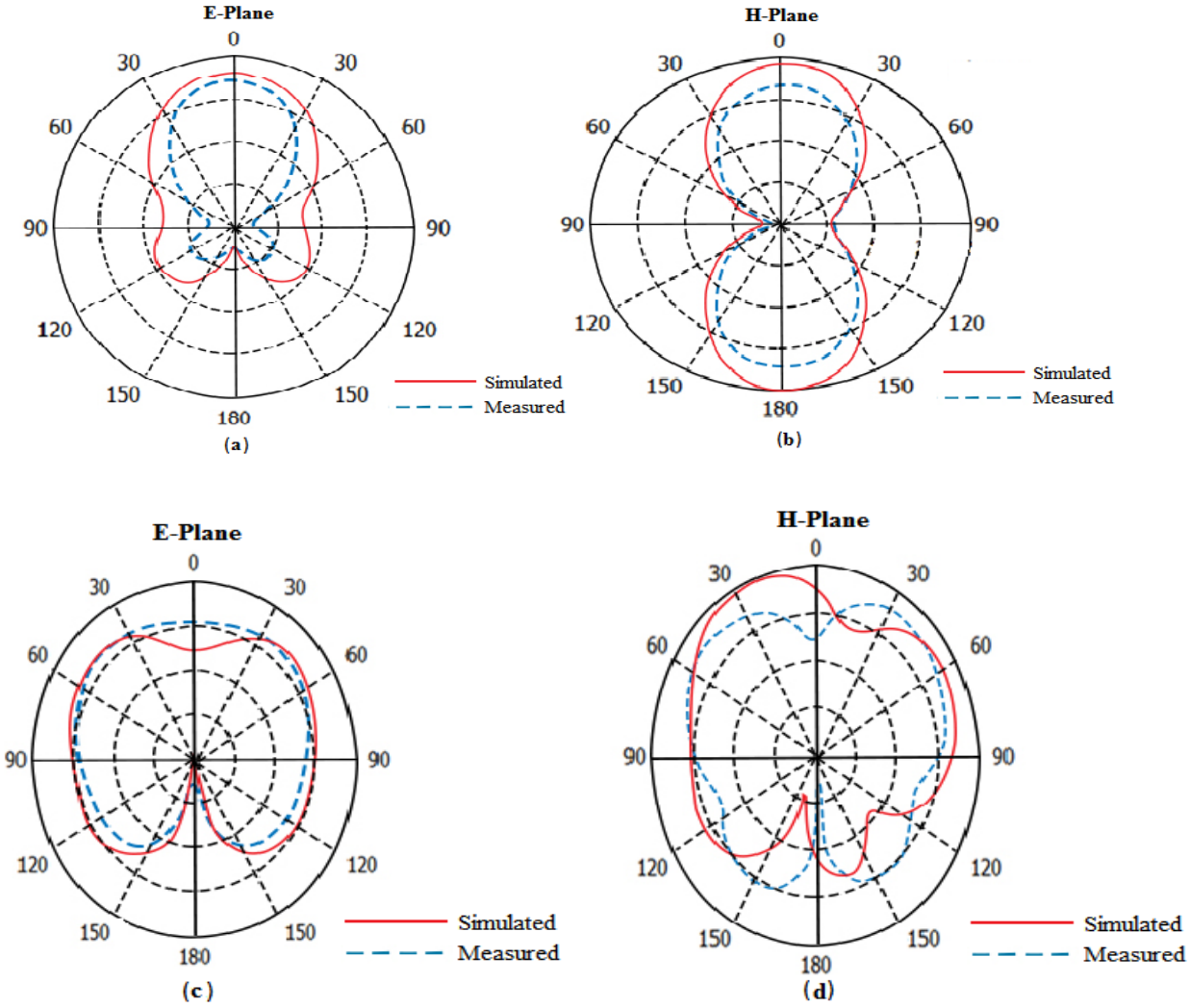

Figure 6.9 Simulated and measured radiation pattern (a-b) 11.47 GHz (c-d) 16.24.

	Bandwidth(GHz) (-10dB)	Resonant Frequencies(GHz)	Level S_{11}(dB)
Measured	11.13-11.82	11.47	-29.61
	15.77-16.89	16.27	-19.76
Simulated	10.90-12.04	11.76	-28.20
	15.06-16.23	15.67	-19.89

Table 6.1 Comparison of measured and simulated results of proposed antenna.

6.5 FABRICATION OF HAND-FAN SHAPED ANTENNA

Figure 6.10 shows the layout for the simulated proposed antenna using Orcad software. This software was used to design desired dimensions of antenna to be fabricated for experimental verifications. After drawing the outline of antenna negative was created. Following the steps that were mentioned in flowchart above PCB was developed for proposed antenna. After final fabrication texting took place. Further Figure 6.11 shows the photograph of fabricated antenna. A connector was connected to the final fabricated antenna for testing. The connector is so selected that it could measure proposed antenna's performance for desired operating frequency.

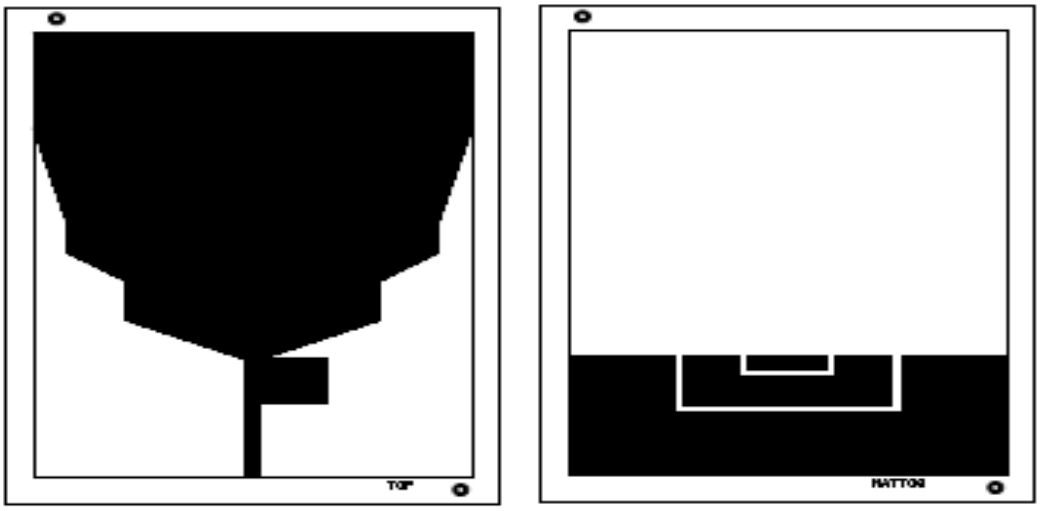

(a) (b)

Figure 6.10 The layout for the simulated proposed antenna using Orcard software (a) top view (b) bottom view.

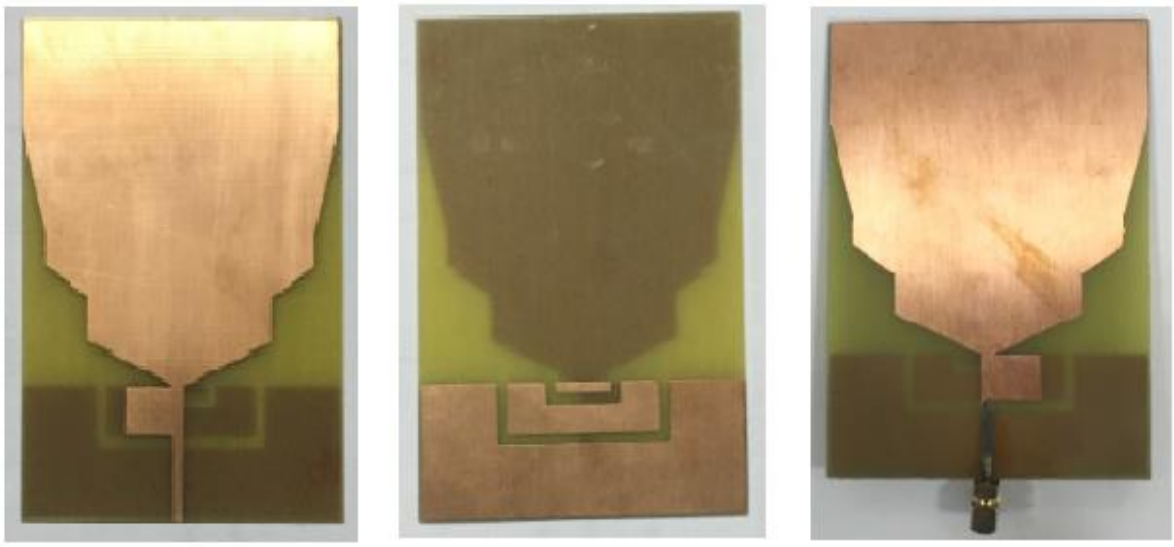

(a) (b) (c)

Figure 6.11 The photograph of fabricated antenna (a) front view (b) back view (c) with connector.

6.5.1 Comparison of Simulated and Measured S-parameter of Proposed Antenna

Figure 6.12 shows the comparison of simulated and measured S-parameter of proposed antenna. It was observed that the measured result covers the frequency range from 0.91 - 2.82 GHz with impedance bandwidth of 1910 MHz that was slightly shifted than the simulated results ranging from 0.94 - 3.05 GHz with impedance bandwidth of 2110 MHz. However, the measured result shows 90% of matching with the simulated results. The proposed antenna covers L-band and S-band ranging from 0.91 - 2.82 GHz. The major reason for this slight variation can be external losses due to cable, inaccurate fabrication process or mismatching of the feedline.

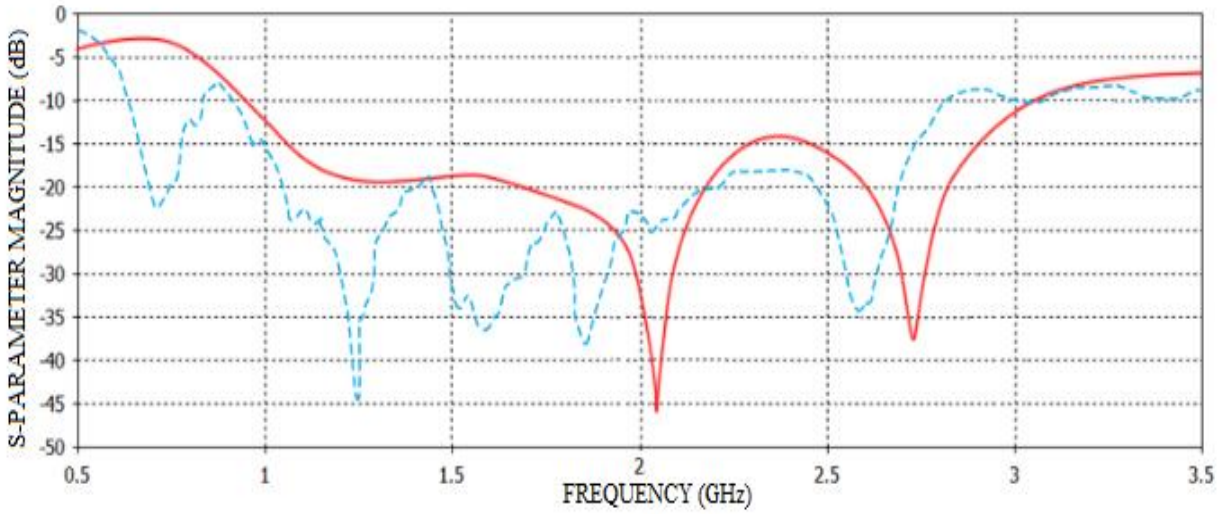

Figure 6.12 The comparison of simulated and measured S-parameter of proposed antenna.

CHAPTER 7

CONCLUSION AND FUTURE SCOPE

CONCLUSION

- In this thesis work a dual-band rectangular, modified t-shape and hand-fan shaped MPAs are represented. A modified t-shape and dual-band rectangular MPAs were optimized using DE algorithm. The DE algorithm is by all accounts a cheerful approach for antenna issues which incorporates improvement and minimization. For these antennas various antenna characteristics are studied such as reflection coefficient, bandwidth, gain, radiation pattern and current distribution.
- Chapter 1 deals with presentation of MPAs and DE algorithm. It covers the problem background together with the goals of the research. The work begins with designing various geometries and feeding techniques of MPAs. Futher various algorithms for optimizing the antenna parameters are discussed. Problem statement and justification of our research work is explained in this chapter.
- Chapter 2 proceeds with the literature survey and work done till today on MPAs and DE algorithm. In this chapter various research work which conclude the gaps in these researches are discussed.
- Next chapter 3 represents a differential algorithm based dual-band rectangular microstrip patch antenna. Differential algorithm (DE) is implemented in this work for optimizing the antenna geometrical design parameters to achieve the desired results. In this paper, on the opposite sides of an inexpensive material FR4 the radiating patch and ground are etched. The slots with various dimensions are etched on both the non-radiating edges of rectangular patch. The ground plane is also been reduced and modified with a slot in it referred to as DGS. These slots are responsible for impedance matching, enhancing bandwidth and for improving antenna radiation characteristics. The microstrip feedline is fabricated on the upper side of the substrate to feed the radiator, which touches the patch on one end, and the other end of the feedline touches the end point of the substrate along its width. The proposed antenna covers dual-frequency bands viz. 2.34 - 2.68 GHz and 5.28- 6.32 GHz with their resonating frequencies at 2.53 GHz and 5.77 GHz respectively, which could be suitable to cover the required bandwidths of Bluetooth (2.4-2.5 GHz), LTE (2.5-2.7 GHz), UMTS-II (2.5-2.7 GHz), ISM & WLAN (2.4–2.484 GHz), Wi-MAX (2.5-2.69

GHz; 5.25-5.85 GHz), WLAN (5.725-5.825GHz), RFID (2.4-2.483 GHz;5.725-5.875 GHz), WiBro (2.3-2.4GHz) and Wi-Fi (5.15-5.825 GHz).

- Chapter 4 represents a modified T-shape microstrip patch antenna using differential algorithm. This work is a demonstration of Differential Algorithm (DE), which is used to optimize the various design parameters of slotted patch antenna in accordance with diverse necessities and scenarios, and also lowers the computation complexity of antenna. The proposed antenna is mounted on a low-loss thin sheet of insulating dielectric substrate named Epoxy Glass-FR4. . On one side, this dielectric is covered with metal generally known as ground and on the other side of the substrate moderately metalized covering is present, which is known as patch and all the antenna patterns are being printed on the patch. The feed line and patch are fabricated on the upper side of the substrate. In this proposed antenna design, inset-cut feed arrangement is used, which is at the depth of approximately half of the length of ground plane, that feeds the radiator. The patch and ground plane has slots etched on them. The proposed antenna covers the frequency range of 11.13-11.82 GHz and 15.77-16.89 GHz with their respective bandwidths of 690 MHz and 1120 MHz with their respective operating frequencies at 11.47 GHz and 16.27 GHz. An inset-cut fed microstrip antenna has been designed and manufactured for the application in the X-band and Ku-band microwave frequency range.
- In chapter 5 hand-fan shaped MPA with double U-slot defected ground structure (DGS) for ultra-wide band (UWB) applications is presented. It is a basic rectangular patch antenna which has gone through number of changes to achieve the desired results. The microstrip feedline which is the least difficult of all the feeding strategies is utilized as a feeding component for this antenna configuration. The radiating material is designed in such a way that it resembles the hand-fan shape structure. Slots s1, s2 and s3 are being expelled from the patch to show signs of improvement in antenna characteristics. The utilization of partial ground and stub in the feedline permits the broadening of the bandwidth and acquiring better impedance matching. The proposed antenna covers the frequency range from 0.91 - 2.82 GHz with impedance bandwidth of 1910 MHz. The obtained frequency range covers the L-band (Telemetry, Aeronautical, military systems for passive satellite sensors) and S- band (weather radars, surface ship radars and communication satellites) applications. Further, the frequency range 2.4 - 2.68 GHz is reserved for SHF RFID, Bluetooth, WiMAX, ISM, WiBro and WLAN applications.

- Chapter 6 deals with the fabrication and testing of proposed antennas that were simulated in Chapter 3, 4 and 5. This is carried out in order to check the applicability of proposed antennas. After the final fabrication of simulated antenna design an appropriate feedline is attached to the proposed antenna for feeding the radiating element. The testing of fabricated antenna is carried out by Aglient E5071C VNA and Anechoic Chamber for reflection coefficient and radiation intensity respectively. The measured results of reflection coefficient for dual band MPA cover the frequency range of 2.34–2.68 GHz and 5.28–6.32 GHz with 340 MHz and 1040 MHz bandwidth respectively and with their respective resonant frequencies at 2.53 GHz and 5.77 GHz. The measured results of reflection coefficient for modified t-shaped MPA covers the frequency range of 11.13-11.82 GHz and 15.77-16.89 GHz with their respective bandwidths of 690 MHz and 1120 MHz and with their respective operating frequencies at 11.47 GHz and 16.27 GHz. The measured results of hand-fan shaped MPA covers the frequency range from 0.91 - 2.82 GHz with impedance bandwidth of 1910 MHz. These frequency ranges cover almost every wireless application.

FUTURE SCOPE

- Some vital regions that require consideration might be appropriately asked into for the future extent of this work to get more profound understanding into the multi frequency MPAs covering different applications. They incorporate enormously small size of antenna components without the loss of efficiency, bandwidth enlargement and enhanced radiation efficiency and gain.
- The electromagnetic energy absorbed by user's head is insignificant as they might cause health risks if user's head is limited by electromagnetic energy on all sides for quite a while. Thus this could be another noteworthy field to study.
- The simulated antennas discussed above in chapter 3, 4 and 5 can be optimized further. This should perhaps be possible by using other algorithms, various thickness, material and dielectric constant for the substrate as well as patches of different dimensions and shapes. Also, by utilizing diverse slots on patch and ground and external networks can also be incorporated into circuits for obtaining multiband and wideband behavior. Other feeding techniques such as coaxial feeding, aperture coupled, proximity coupling and CPW can also be used for designing same MPAs.

- We can likewise utilize meta-material to outline antennas: A meta-material is a metallic or semiconductor substance whose properties rely upon its inter-atomic structure instead of on the synthesis of the atoms themselves. Certain meta-materials bend visible light beams in the inverse sense from customary refractive media. Some meta-materials additionally display such conduct at infrared (IR) wavelengths. Conceivable utilizations of transparent meta-materials with negative indices of refraction incorporate red and IR lasers, optical communication systems, spectrometry etc.
- The DGS has been examined experimentally for dual band/multiband/multi frequency operations in antenna. A numerical as well as unquestionable model can likewise be designed for a particular DGS structure for specific application of antenna.

REFERENCES

[1] Wentworth S.M. (2005). *Fundamentals of Electromagnetics with Engineering Applications*, John Wiley & Sons, NJ, USA.

[2] Garg R., Bhartia P., Bahl I. and Ittipiboon A. (2001). *Microstrip Antenna Design Handbook*, Norwood, MA: Artech House.

[3] Deschamps G.A. (1953). *Microstrip Microwave Antennas*, 3rd USAF Symposium on Antennas. University of Illinois, Urbana.

[4] Gutton H. and Baussinot G. (1955). *Flat Aerial for Ultra High Frequencies*, French Patent No. 703113.

[5] Sainati R.A. (1996). *CAD of Microstrip Antennas for Wireless Applications*, The Artec House Antenna Library.

[6] Chang k. (2000). *RF and Microwave Wireless Systems*, New York, NY: Wiley.

[7] Balanis C.A. (2015). *Antenna Theory Analysis and Design*, New York, NY: Wiley.

[8] Kara M. (1998). Design Considerations for Rectangular Microstrip Antenna Elements with Various Substrate Thicknesses, *Microwave and Optical Technology Letters*, 19 (2), 111-121.

[9] Guney K. and Sarikaya N. (2009). Comparison of adaptive-network-based fuzzy inference systems for bandwidth calculation of rectangular microstrip antennas, *Expert Systems with Applications*, 32(2), 3522–3535.

[10] Singh I. and Tripathi V.S. (2011). Microstrip Patch Antenna and its Applications: A Survey, *International journal of computer technology and application*. 2(2), 595-1599.

[11] Guney K. and Sarikaya N. (2006). Adaptive Neuro-Fuzzy Inference Systems for Computation of the Bandwidth of Electrically Thin and Thick Rectangular Microstrip Antennas, *Electrical Engineering Journal*, 88(3), 201–210.

[12] Saeed R. and Khatum S. (2005). Design of Microstrip Antenna for WLAN, *Journal of Applied Sciences*, 5(1), 47-51.

[13] Arunachalam V. (2008). *Optimization using Differential Evolution*, The University Of Western Ontario, London, Ontario, Canada.

[14] Zhang H., Wang Z., Yu J. and Huang J. (2008). A Compact MIMO Antenna for Wireless Communication, *IEEE Antennas and Propagation Magazine*, 50(6), 104-107.

[15] Kaur J., Khanna R. and Kartikeyan M.V. (2014). Optimization and Development of O-shaped Triple-band Microstrip Patch Antenna for Wireless Communication Applications, *International Journal of Microwave and Wireless Technology*, 60(2), 95-105.

[16] Shambavi K. (2007). Gain and Bandwidth and Enhancement Technique in Square Microstrip Antenna for WLAN Applications, *Proceedings of Asia-Pacific Microwave Conference*,[Bangkok, Thailand: 2007], pp.1-4.

[17] Dheyab A. and Hamad K. (2011). Improving Bandwidth of Rectangular Patch Antenna using Different Thickness of Dielectric Substrate, *ARPN Journal of Engineering and Applied Sciences,* 6(4), 16-21.

[18] Liu W.C., Wu C.M. and Dai Y. Design of triple-frequency microstrip-fed monopole antenna using defected ground structure, *IEEE Transaction on Antennas and Propagation*, 59(7), 2457–2463.

[19] Agarwal N., Dhubkarya D.C. and Mittal R. (2011). Designing & Testing of Rectangular Microstrip antenna operating at 2.0 GHz using IE3D, *Global Journal of Reseach in Engineering,* 11(1), 44-48.

[20] Kaur J., Khanna R. and Kartikeyan M.V. (2014). Novel dual-band multistrip monopole antenna with defected ground structure for WLAN/IMT/ BLUETOOTH/WiMAX applications, *International Journal of Microwave and Wireless Technology,* 6(2), 93-100.

[21] Karli R. and Ammor H. (2015). Rectangular Patch Antenna for Dual-Band RFID and WLAN Applications, *Wireless Personal Communications*, 83(2), 995–1007.

[22] Kaur A. (2015). Semi Spiral G-shaped Dual Wideband Microstrip Antenna with Aperture feeding for WLAN/WiMAX/U-NII Band Applications, *International Journal of Microwave and Wireless Technology,* 8(6), 931-941.

[23] Chen H.M. (2002). Microstrip-fed dual-frequency printed triangular monopole. *Electronics Letter,* 38(13), 619–620.

[24] Li F. et al. (2010). Compact triple-band monopole antenna with C-shaped and S-shaped meander strips for WLAN/WIMAX applications, *Progress in Electromagnetics Research Letters*, 15, 107–116.

[25] Yassen M. T. et al. (2013). A new compact slot antenna for dual-band WLAN applications, *International Journal of Science and Modern Engineering,* 1(10), 28–32.

[26] Panda J. R. and Kshetrimayum R. S. (2011). A printed 2.4 GHZ/5.8 GHz dual-band monopole antenna with a protruding stub in the ground plane for WLAN and RFID applications, *Progress in Electromagnetics Research Letters*, 117, 425–434.

[27] Anguera, J. et al. Advances in antenna technology for wireless handheld devices, *International Journal of Antennas and Propagation*, 2013, 1–254.

[28] Naji D. K. and Mohammed A. A. (2013). A dual-band U-slot PIFA antenna with ground slit for RFID applications, *Journal of Emerging Trends in Computing and Information Science*, 4(2), 213–220.

[29] Zhong M., Yang S. and Nie Z. (2008). Optimization of a Luneberg Lens Antenna Using the Differential Evolution Algorithm, *IEEE Antennas and Propagation Society International Symposium* [San Diego, CA, USA: 2008], pp. 1-4.

[30] Herscovici N., Osorio M. and Piexeiro C. (2001). Minimization of a rectangular patch using genetic algorithms, *IEEE Transaction on Antennas and Propagation*, 4, 34–37.

[31] Chowdhury A. et al. (2010). Optimization of antenna configuration with a fitness-adaptive differential evolution algorithm, *Progress in Electromagnetics Research B,* 26, (26), 291-319.

[32] Deb A., Roy J.S. and Gupta B. (2011). Design of a probe-fed microstrip antenna using differential evolution algorithm, *IEEE International Symposium on Microwave, Antenna, Propagation and EMC Technologies for Wireless Communications* [4th: Beijing, China: 2011], pp. 46-49.

[33] Tanabe R. and Fukunaga A. (2011). Success-History Based Parameter Adaptation for Differential Evolution, *IEEE Congress on Evolutionary Computation*, 15(1), 4-31.

[34] Zhao, W.J. et al. (2013). A Differential Evolution Based Equivalent Source Approach for Predicting Electromagnetic Emission Using Near-Field Scanning, *IEEE International Symposium on Electromagnetic Compatibility* [11th: Denver, CO, USA: 2013], pp. 182-186.

[35] Deb A., Roy J.S. and Gupta B. (2014). Performance Comparison of Differential Evolution, Genetic Algorithm and Particle Swarm Optimization in Impedance Matching of Aperture Coupled Microstrip Antennas, *IEEE Transaction on Antennas and Propagation*, 62(8), pp. 3920-3928.

[36] Gangopadhyaya M. et al. (2015). IEEE Design Optimization of Microstrip fed Rectangular Microstrip Antenna Using Differential Evolution Algorithm, *IEEE International Conference on Recent Trends in Information System* [2th: Kolkata, India: 2015], pp. 49-52.

[37] Kumar T.A. and Singh B.K. (2013). A CPW feed X- band antenna for satellite and radar application, *International Conference on Microwave and Photonics* [Dhanbad, India: 2013], pp. 1-3.

[38] Singh R. and Singh V.K. (2017). Wide Band and Miniaturized Partial Ground Plane Microstrip Antenna for X & Ku Band Applications, *International Journal of Computer Technology and Applications*, 10(8), 477-486.

[39] Thi T.N., Hwang K.C. and Kim H.B. (2013). Dual-band circularly-polarised Spidron fractal microstrip patch antenna for Ku-band satellite communication applications, *Elecronics Letters*, 49(7), 444-445.

[40] Khandelwal M.K. et al. (2013). Design and Analysis of Microstrip DGS Patch Antenna with Enhanced Bandwidth for Ku Band Applications, *International Conference on Microwave and Photonics* [Dhanbad, India: 2013], pp. 1-4.

LIST OF PUBLICATIONS

PAPERS UNDER REVIEW

- Nitika and Kaur J. (2017). Differential Algorithm based Dual-band Rectangular Antenna for Wireless Applications, *International Journal of Microwave and Wireless Technologies*.
- N., Kaur J. and Khanna R. (2017). Optimization of Modified T-Shape Microstrip Patch Antenna using Differential Algorithm for X and Ku Band Applications*, Microwave and Optical Technology Letters.*

PAPER UNDER WRITING

- Hand-fan Shaped microstrip patch antenna with U-slot DGS for L-band and S-band applications.

ACKNOWLEDGEMENT

It is my proud privilege to acknowledge and extend my gratitude to several people who helped me directly or indirectly in completion of this report. I express my heart full indebtedness and owe a deep sense of gratitude to my teacher and my faculty guides **Dr. Jaswinder Kaur, Assistant Professor,** for their sincere guidance and support with encouragement to go ahead.

I am also thankful to **Dr. Alpana Agarwal**, Professor and Head, ECED, for providing us with the adequate infrastructure for carrying out the work. I am also thankful to **Dr. Hemdutt Joshi,** Associate Professor & P.G. Coordinator, ECED, for the motivation and inspiration and that triggered me for the work.

I would also like to thank my entire friends who have more or less contributed to the preparation of this report. Last but not the least, I would like to thank my parents for their years of unyielding love and encourage. They have always wanted the best for me and I admire their determination and sacrifice. The study has indeed helped me to explore knowledge and avenues related to my topic and I am sure it will help me in my future.

Nitika
(801563018)